Ja'farawy *et al.*
Journal of Analytical Science and Technology (2023) 14:29
https://doi.org/10.1186/s40543-023-00393-2

Journal of Analytical Science and Technology

REVIEW

Open Access

Graphene quantum dot nanocomposites: electroanalytical and optical sensor technology perspective

Muhammad Shalahuddin Al Ja'farawy[1,2†], Dinakaran Thirumalai[3†], Jaewon Lee[3], Ho Sang Jung[1], Seung-Cheol Chang[4*], Jang-Hee Yoon[5] and Dong-Ho Kim[1,2*]

Abstract

Electroanalytical and optical techniques are widely used in the development of nanomaterials-based sensor platforms. These techniques have a quick response, high sensitivity, and selectivity. Electroanalytical and optical techniques are widely used in the development of nanomaterial-based sensor platforms. These sensors must be able to detect biomarkers, pathogens, toxins, and pharmaceuticals in biological matrices associated with cardiovascular disease, cancer, and neurodegenerative diseases. Considering these pathophysiologies, numerous investigations have been undertaken to develop sensors for early diagnosis and treatment, utilizing nanomaterials such as quantum dots. Graphene quantum dots (GQDs), which are ideally nanometer-sized graphene fragments, have recently received increased attention due to their excellent physicochemical properties such as fast electron mobility, photostability, water solubility, biocompatibility, high specific surface area, and nontoxicity. Apart from the properties mentioned above, GQDs provide π–π interactions, electrostatic, and covalent interactions with an analyte, and ease of synthesis as well as the ability to combine with other nanomaterials, which have enabled their use in various sensing platforms. This review summarizes recent advances in GQDs-based nanocomposites for sensor applications, with a focus on electroanalytical and optical techniques, as well as current challenges and future prospects.

Keywords Graphene quantum dots, Nanocomposites, Electroanalytical sensor, Optical, Electrochemical, Biosensors

†Muhammad Shalahuddin Al Ja'farawy and Dinakaran Thirumalai contributed equally to this work.

*Correspondence:
Seung-Cheol Chang
s.c.chang@pusan.ac.kr
Dong-Ho Kim
dhkim2@kims.re.kr
[1] Nano-Bio Convergence Department, Korea Institute of Materials Science, Changwon, Gyeongnam 51508, Republic of Korea
[2] Advanced Materials Engineering Division, University of Science and Technology (UST), 217 Gageong-ro, Yuseong-gu, Daejeon 34113, Republic of Korea
[3] BIT Convergence-Based Innovative Drug Development Targeting Meta-Inflammation, Department of Pharmacy, College of Pharmacy, Pusan National University, Busan 46241, Republic of Korea
[4] Department of Cogno-Mechatronics Engineering, College of Nanoscience and Nanotechnology, Pusan National University, Busan 46241, Republic of Korea
[5] Busan Centre, Korea Basic Science Institute, Busan 46742, Republic of Korea

Introduction

Electroanalytical chemistry is a cutting-edge field of electrochemistry, also known as electroanalysis, that focuses on the development of new techniques, and modified electrodes for quantitative analytical investigations that can be used to detect and sense an analyte. This technology has a wide range of applications including better understanding and monitoring of blood glucose levels (Minteer 2018).

Many studies using electroanalytical techniques have focused on the development of a tool for the diagnosis of many diseases over the last few decades. Electroanalytical techniques combined with nanotechnology have proven to be excellent models for both in vivo and in vitro quantitative biomolecule analysis. Multiple biomolecules can be detected using electroanalytical sensors. They have received a lot of attention due to their advantageous characteristics such as ease of use, rapid response time, excellent sensitivity, dynamic linear concentration range, cost-effectiveness, real-time detection, and miniaturization capability.

Apart from electroanalytical methods, optical detection approaches have emerged as promising sensing techniques, particularly for in vivo measurements of biomolecules. Because of their advantages, optical sensors have proven to be highly effective. Their reproducibility and sensitivity tend to be significant. Furthermore, their detection limit is frequently in the nanomolar range or less. Using the optical spectrum over a wide range can also reduce interference from other biological compounds (Eddin and Fen 2020).

Qualitative and quantitative analyses of target analytes in pathogen detection, and medical diagnostics require sensitive, rapid, and effective biosensors (Kaur et al. 2015; Wadhera et al. 2019). Biosensors provide information regarding bio-compositions, structures, and functions of analytes through electrical, or optical signals (Guo 2012; Nguyen et al. 2019; Pirzada and Altintas 2019). Various biosensors have been developed since 1956 and are being improved to penetrate broad markets and specializations (Goode et al. 2015; Sireesha et al. 2018).

Recent advances in nanotechnology have shown considerable promise in developing ultrasensitive biosensors with femto-, pico-, and nanosensitivity, which are essential to meet the demand and develop highly specific and sensitive diagnostics (Iannazzo et al. 2021; Liang et al. 2021). Compared to conventional screening techniques such as enzyme-linked immunosorbent assays, novel biosensing technologies have a greater potential to overcome limitations such as real-time analysis, low limits of detection (LOD), and high-throughput screening (Iannazzo et al. 2021; Pirzada and Altintas 2019; Sharifi et al. 2019). Owing to their small size, nanomaterials in the range of 1–100 nm often enhance the repeatability, selectivity, and sensitivity of biosensors, setting them apart from bulk materials in regard to fundamental physicochemical features (Iannazzo et al. 2021; Pirzada and Altintas 2019).

Nanomaterials are classified as carbon allotrope nanomaterials, inorganic nanomaterials (metallic and nonmetallic materials), and organic materials (polymeric nanomaterials) based on their chemical compositions (Pirzada and Altintas 2019). Recently, carbon nanomaterials have received increasing attention as materials in biosensing applications owing to their characteristic properties such as high surface area, high carrier transport mobility, excellent mechanical flexibility, excellent thermal and chemical stability, and unique optical properties. Graphene quantum dots (GQDs), exhibiting tunable photoluminescence (PL), were identified among carbon nanomaterials as zero-dimensional (0D) graphene sheets of quantum size < 10 nm (Liang et al. 2021; Xie et al. 2016). GQDs are different from graphene, which does not exhibit photoluminescence behavior in a pristine state owing to a zero optical bandgap (Hai et al. 2018). Furthermore, GQDs exhibit excellent biocompatibility, low cytotoxicity, and good resistance to photobleaching as compared to conventional fluorescent molecules and semiconductor quantum dots, which face photobleaching and biocompatibility challenges (Li et al. 2013b; Xie et al. 2016). The unique physical and chemical properties of GQDs have afforded the rapid development of GQDs-based nanocomposites, particularly in biosensing applications.

In this review, we discuss the potential benefits of using GQDs-based nanocomposites in electroanalytical and optical sensing platforms (Fig. 1), including recent advancements and future perspectives. We have mainly focused on voltammetric, amperometric, and impedimetric sensors in the electroanalytical part and surface-enhanced Raman scattering (SERS), and fluorescence sensors in the optical part that are fabricated using GQDs-based nanocomposites.

Characteristics of graphene quantum dots

Structural properties

GQDs are 0D carbon-based materials comprising several graphene flakes with dimensions < 20 nm and a height of a few nanometers (Choi 2017; Facure et al. 2020; Zhang et al. 2019). GQDs are nonzero bandgap materials exhibiting the quantum confinement effect (Tabish and Zhang 2016). The small size of GQDs makes quantum confinement dominant, and the Coulomb blockade peaks are unequally spaced instead of being periodically distributed (Perini et al. 2020). This quantum confinement effect is induced by the particle size of GQDs as well as by chirality, boundaries, and shape of the edges, all of which

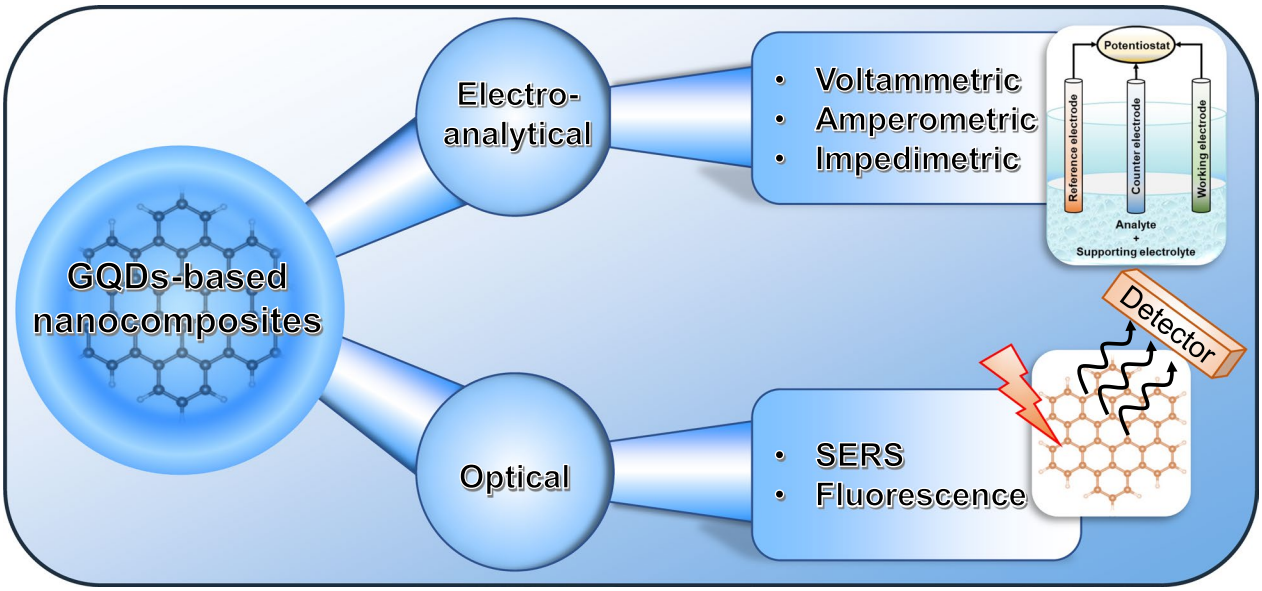

Fig. 1 Infographic illustration of graphene quantum dots (GQDs) for electroanalytical and optical sensor applications

depend on the synthesis methods of GQDs (Choi 2017; Perini et al. 2020; Zhang et al. 2019).

Several studies have reported that GQDs can be elliptical, triangular, quadrate, and hexagonal, as shown in Fig. 2a (Zhang et al. 2019; Zheng et al. 2015; Facure et al. 2020). The elliptical shape of GQDs is the most popular owing to minimizing edge-free energies and the reconstruction of crystallization (Dai et al. 2014). According to Kim et al. (2012), the different shapes of GQDs exhibit variable average sizes. For instance, circular and elliptical GQDs exhibit typical sizes of ~ 5 nm and 12 nm. Size-dependent are related to the optical properties of GQDs, such as PL, in which increasing particle size of GQDs will shift the PL emission wavelength from the blue region into the red region (Sk et al. 2014).

The size-dependent optical properties are related to the bandgap energy of GQDs. As shown in Fig. 2b, increasing the particle size of GQDs will narrow down the bandgap energy. Reshma and Mohanan (2019) explained that the bandgap energy depends on the distance between electron–hole pairs due to the squeezing of electron–hole pairs. The smaller size of GQDs results in more squeezing of electron–hole pairs that leads to higher energy levels, while the unpaired electrons from the functional groups on the surface of GQDs will contribute to the electron donation from the functional groups into the GQDs based on the electron-withdrawing and electron-accepting behaviors of functional groups. As a result, increasing the electron density will lower the bandgap energy which has a similar tendency to be size-dependent (Jin et al. 2013; Yan et al. 2018).

Optical properties

GQDs typically exhibit strong optical absorption in the ultraviolet (UV) region around 230–320 nm, with an absorption shoulder extending into the visible region, as shown in Fig. 2c (Zhuo et al. 2012; Ghosh et al. 2021; Zhang et al. 2019; Zhu et al. 2015). These absorption spectra are related to a specific electronic structure determined by π–π^* transitions within the aromatic rings, sp^2-hybridized portions, and lone pairs within oxygens (Haque et al. 2018; Perini et al. 2020). For instance, the absorption peak around ~ 230 nm occurs due to the π–π^* transition of phenyl rings and aromatic C=C bonds, whereas the absorption shoulder at ~ 300 nm is attributed to the n–π^* transition of C=O bonds or other moieties (Li et al. 2013a, 2019a, Ozhukil Valappil et al. 2017).

GQDs exhibit tunable PL properties ranging from UV to visible, depending on the excitation wavelength, as shown in Fig. 2d (Zhuo et al. 2012; Choi 2017). The small particle size of GQDs affords a quantum confinement effect, yielding bandgap energy and PL on excitation (Facure et al. 2020; Perini et al. 2020). Theoretically, the bandgap energy of GQDs should not exceed 1.0 eV as the size is limited to several nm (Choi 2017). However, several experiments have reported that the PL energy of GQDs has been observed to be ~ 3.0 eV (Shen et al. 2011). According to Liu et al. (2010), this phenomenon might occur due to electron–phonon scattering, which minimizes thermalization, as observed in the case of pristine graphene without bandgap energy. Kim et al. (2012) showed that this PL emission could

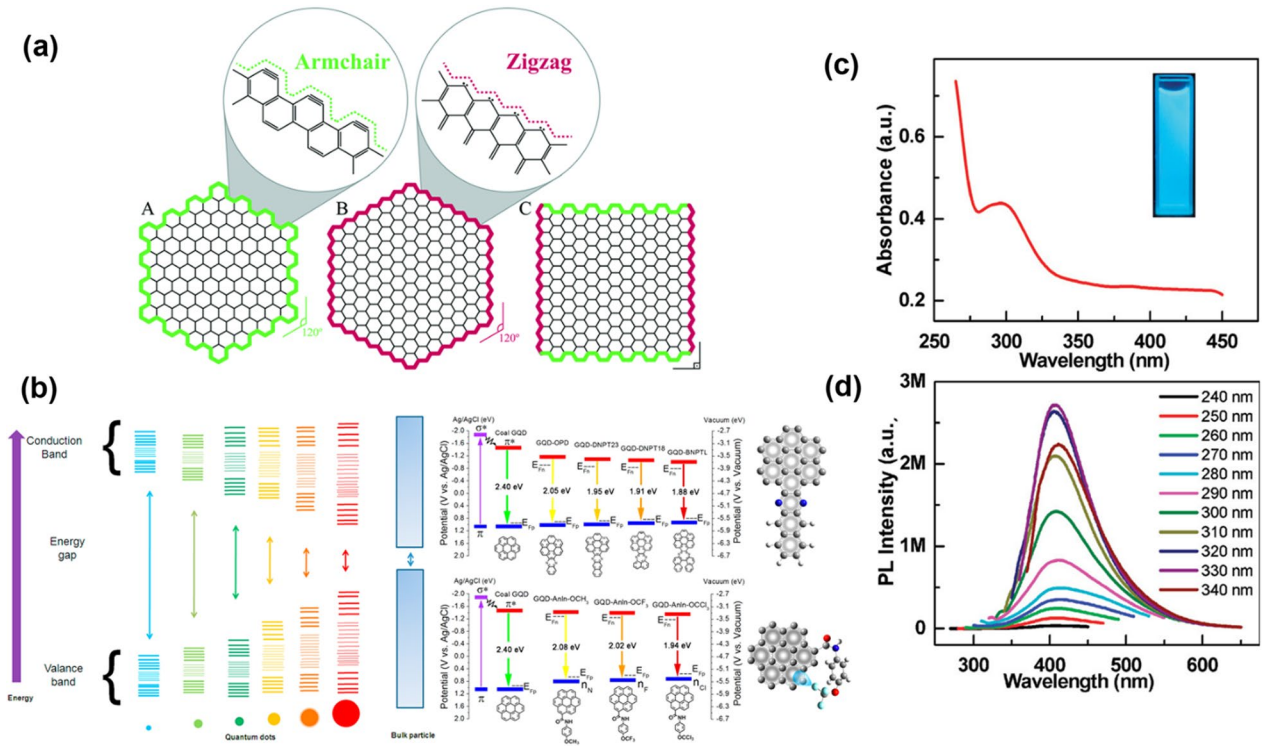

Fig. 2 **a** The shape of GQDs in different types of edges (Reproduce with permission from Reference Facure et al. 2020, Copyright 2020, Royal Society of Chemistry), **b** Illustration of bandgap energy mechanism of GQDs based on confinement size (Reproduce with permission from Ref. Reshma and Mohanan 2019, Copyright 2019, Elsevier) and surface functional group (Reproduce with permission from Ref. Yan et al. 2018, Copyright 2018, American Chemical Society), **c** UV–Vis absorption spectra of GQDs, **d** Photoluminescence spectra of GQDs under different excitation wavelengths (Reproduce with permission from Ref. Zhuo et al. 2012, Copyright 2012, American Chemical Society)

be controlled by modifying the size and edge of GQDs, thereby altering the electronic transitions in GQDs.

In addition to excellent PL properties, GQDs exhibit a superior PL quantum yield (PLQY) than carbon dots (CDs), which have a poor PLQY value (~ 10–15%) owing to the traps on the surface (Ghosh et al. 2021; Zhu et al. 2011). The high PLQY of GQDs is related to their layered structure and crystallinity (Ghosh et al. 2021). Several studies have shown that QY highly depends on surface passivation, explaining why GQDs have a greater PLQY than CDs. The high PLQY of GQDs is ascribed to the self-passivation that occurs during the synthesis of GQDs. According to Haque et al. (Haque et al. 2018), GQDs passivated with a hydrogen atom on their edges exhibited a poor QY, indicating the disadvantage of hydrogen in passivating the surface (Mueller et al. 2010). When passivated with carbonyl, epoxy, and other functional groups, GQDs exhibited improved PLQY and PL lifespan (Haque et al. 2018; Wang et al. 2016).

Chemical properties

Owing to the presence of oxygen functional groups on their surface, GQDs can act as reducing agents (Kappen et al. 2021; Sinduja and John 2019; Thanomsak et al. 2021). They can reduce metal precursors into metal particles under a certain molar ratio of GQDs (Ge et al. 2016; Liu et al. 2017b). The hydroxyl groups on the surface of GQDs are considered reductive groups. They are transformed into carbonyl groups after the reduction of metal ions, forming metal nanoparticles on the surface of GQDs (Thanomsak et al. 2021). According to Jin et al. (2022), the excellent electron-donating capability of GQDs from the abundant –OH and $–NH_2$ groups enables a fast reduction of the metal precursor into metal nanoparticles via electron transfer. Xiaoyan et al. (2016) reported that the hydroxyl groups easily fall off the graphene sheets owing to the breaking of the C–O bond, which yields a strong reducing ability. The abundant oxygen functional groups on the surface of GQDs make them nucleation centers for the nucleation and growth of metal nanoparticles (Wu et al. 2016).

GQDs are ideal for replacing toxic capping agents in the synthesis of metal nanoparticles (Jin et al. 2022; Sinduja and John 2017). They help keep metal particles stable by preventing aggregation and oxidation. Metal ions are attracted to the surface of GQDs via electrostatic

interactions with abundant functional groups. On heating, the interfacial junction allows more electron transfer from the GQDs to the metal ions, forming conductive metal nucleation sites and eventually promoting the growth of metal particles. Meanwhile, the growth of metal particles will attract more GQDs to serve as capping agents on their surfaces (Guo 2012; Jin et al. 2022).

Biocompatibility properties

In addition to excellent their structural, chemical, and physical properties, GQDs exhibit strong biocompatibility, which is crucial in bio-applications (Biswas et al. 2021; Chandra et al. 2014). Generally, the degradation of GQDs does not produce any toxic substance harmful to living organisms (Chandra et al. 2014). GQDs are different from traditional semiconductor quantum dots (QDs), which exhibit intrinsic toxic properties owing to the side product of heavy-metal components. The QDs also cause apoptosis in living organisms, which is related to their oxidative stress (Biswas et al. 2021). Thus, QDs cannot be used in biomedical applications.

Several studies have shown that ultrasmall particles of GQDs (< 6 nm) may cause cell apoptosis as they can enter the mitochondria and cause physical damage, contributing to oxidative stress. However, according to Sapkota et al. (2017), the cytotoxicity of GQDs is dependent on their size. Shang et al. (2014) reported that sub-10 nm nanoparticles are more toxic to living cells than larger particles as smaller particles can freely diffuse to the nucleus (Sapkota et al. 2017; Zhang et al. 2014). Wu et al. (2013) showed that GQDs exhibited low cytotoxicity in gastric and breast cancer cells compared to micrometer-sized graphene oxide (GO).

To get high biocompatibility of GQDs, several factors should be considered. (1) The precursor and solvent must be nontoxic (for instance, they should only produce GQDs, water, or carbide precipitates); (2) the edge structure and the functional group of GQDs should be similar to living cell components such as glucose, which is the energy source of living cells and the intermediate product of metabolism (Yan et al. 2019). According to Umrao et al. (Umrao et al. 2015), the synthesis process involving complicated and harmful chemicals might cause GQDs to have oxygen functional groups, which affects the cytotoxicity of the GQDs. On the other hand, the presence of oxygen functional groups can enhance PL emission and chemisorption which is beneficial in biosensing applications. Several reports have suggested balancing the oxygen content of the GQDs to provide high PL emission and low cytotoxicity (Lee et al. 2020).

Role of GQDs in biosensing

Capturing agent

The adsorption of the target analyte onto the surface, which is related to the interaction between the analyte and the biosensor surface, is crucial to the performance of a biosensor (Bell et al. 2020). To improve the selectivity of biosensors, the binding affinity between the analyte and the surface should be observed via physisorption (electrostatic, π interactions, hydrogen bond, and van der Waals forces) and chemisorption (covalent bond interaction) (Perez-Jimenez et al. 2020). Noble metals are usually used as probes or substrates of biosensors. However, the adsorption ability of analytes onto the surface can be restricted by the poor affinity of some target molecules toward the metal surface (Miao et al. 2019).

To address this challenge, carbon nanomaterials, including GQDs, were introduced onto the surface of the metal to promote the adsorption of the target molecule. Prasad et al. (Bali Prasad et al. 2017) reported that graphene-based materials are the new "miracle material" in various applications, including biosensors. The good performance of GQDs is attributed to a large surface-to-volume ratio correlated with multiple molecule recognition sites (Facure et al. 2021). The large surface area of GQDs yields a high probability of target molecules contacting the surface (Ge et al. 2016). Furthermore, functionalized groups on the surface of GQDs and the π-conjugate plane structure are advantageous for interacting and adsorbing target molecules on edge sites (Cheng et al. 2012; Facure et al. 2020). GQDs containing rich-oxygen functional groups have a negative charge on their surface, which attracts target molecules via electrostatic interactions (Cheng et al. 2012). In principle, removing functional groups from the surface of GQDs induces a more pronounced sp^2-hybridization character, yielding low electrical resistance. However, Facure et al. (2021) explained that the maintenance of functional groups is beneficial to the interaction of analytes.

Adding functional groups can further improve the hydrophobicity of GQDs, promoting their potential to deliver insoluble molecules (Liaquat et al. 2022; Pinilla-Penalver et al. 2022). Generally, the strong hydrophobic nature of graphene-based materials may deter analyte recapture in an aqueous solution owing to interfacial resistance (Bali Prasad et al. 2017). Furthermore, the carboxylic moieties at the edge of GQDs help water dispensability, where their functional groups could be easily complexed with several compounds, including inorganic, organic, polymer, or biological compounds. According to Prasad et al. (Bali Prasad et al. 2017), the hydrophilic edges and the hydrophobic plane in GQDs increase analyte absorption. The introduced functional groups on the surface of GQDs can also improve molecular recognition

properties (Facure et al. 2021). Practically, some recognition molecules with high selectivity for specific target molecules can be adopted. For instance, Wei et al. (2014) used cyclodextrins with GQDs as nanocomposites to enhance supramolecular recognition capability. Huang et al. (2016) explained that the primary π-network at the surface of GQDs acts as a recognition receptor owing to strong $\pi-\pi$ stacking interactions and electrostatic adhesion. The rich amino groups on the surface of GQDs attract biochemical molecules via electrostatic interactions and $\pi-\pi$ stacking interactions (Liu et al. 2018b).

Fluorescence agent

Owing to their simple preparation, minimal reagents, easy functionalization, and excellent fluorescence properties, GQDs can be used as fluorescence platforms in various biological applications, such as labeling, diagnostic, drug delivery, and electronic devices for health monitoring (Garg et al. 2021; Ryu et al. 2015). GQDs have been widely used to investigate analytes such as pesticides, metal ions, organic pollutants, food adulterants, bacterial spores, and nucleic acids owing to their PL properties, pH-sensitive luminescence, and up-conversion PL properties (Fan et al. 2017; Garg et al. 2021; Wang et al. 2013). Furthermore, GQDs have high brightness and photostability against photobleaching, which is suitable for fluorescence applications. The optical properties of GQDs are different from organic dyes and semiconductor QDs that suffer from photobleaching (Salehnia et al. 2017; Sapkota et al. 2017).

GQDs exhibit a narrow, almost symmetrical fluorescence spectrum with a strong emission peak at 447 nm under 345 nm excitation (Huang et al. 2015). Notably, the fluorescent behavior of GQDs is dependent on the excitation wavelength. With increasing excitation wavelength, the emission peak of GQDs shifts to a longer wavelength, and fluorescence intensity initially becomes strong and subsequently weakens (Huang et al. 2015; Tang et al. 2014).

GQDs-based nanocomposite for biosensing

Electroanalytical sensors

GQDs are preferred in electrochemical sensors owing to their oxygen-rich functional groups, excellent quantum confinement, edge effects, stability, biocompatibility, large surface area, ease of production process, and ability to be doped or modified for specific biosensing applications. Thus, GQDs-based electrochemical sensors have low LOD and high sensitivities. In many cases, GQDs can be combined with other nanomaterials to develop GQDs-based nanocomposites with synergistic effects to promote catalytic reactions with target analytes (Campuzano et al. 2019; Ji et al. 2020; Li et al. 2019b; Mansuriya and Altintas 2020; Tabish et al. 2021; Tajik et al. 2020).

GQDs-based nanocomposites for voltammetric sensors

Voltammetry is a common transduction technique used in the development of electroanalytical sensors. It allows for sensitive and fast quantitative analysis of redox-active analytes, as well as the characterization of the electrochemical process occurring on the surface of the sensing electrode. Additionally, voltammetry can offer simultaneous determination of different interfering substances. Among all voltammetric methods, differential pulse voltammetry (DPV), square-wave voltammetry (SWV), cyclic voltammetry (CV), and linear sweep voltammetry (LSV) are the most preferred techniques for the detection of small molecules, and proteins (Xu et al. 2017).

Several GQD-based nanocomposites have been successfully prepared using various approaches for detecting small molecules. Small molecules such as metabolites, vitamins, hormones, cofactors for proteins, and intracellular messengers play a vital role in the human body. It is possible to diagnose, monitor, and predict illness progression by quantifying the concentration of small molecules associated with a specific disease (Facure et al. 2021).

Uric acid (UA), a by-product of purine metabolism in the liver, is found in body fluids such as blood, urine, and sweat. Monitoring the UA level in body fluids is essential because it can strongly indicate renal disease. Wang et al. (2022) developed enzyme-free wearable sensors, and the DPV technique was used to monitor UA concentrations in human sweat using boron-doped GQDs attached to carbon nanotubes (BGQDs/CNTs) as noble metal-free electrocatalysts (Fig. 3). BGQDs can provide additional active sites to improve the electrocatalytic ability of the UA oxidation reaction. According to density functional theory calculations, boron atoms can improve UA adsorption and increase electron transfer from the UA to the B-doped graphene sheet, which supports the high sensitivity of BGQDs for UA detection. Yola and Atar (2018) constructed a novel molecularly imprinted sensor on GQDs with two-dimensional (2D) hexagonal boron nitride nanosheets (2D-hBN) for detecting serotonin (SER) in urine samples. They claimed that the molecular imprinting approach has a high selectivity for detecting SER. According to Ahmadi et al. (2020), novel electrochemical and photoelectrochemical dopamine (DA) sensors were developed using titania–ceria–graphene QD (TC–GQD) nanocomposites. They noticed that the electrical conductivity and bandgap of the TC–GQD nanocomposite were considerably improved owing to the synergistic effect of the nanocomposite components toward DA detection. Similarly, GQDs with gold

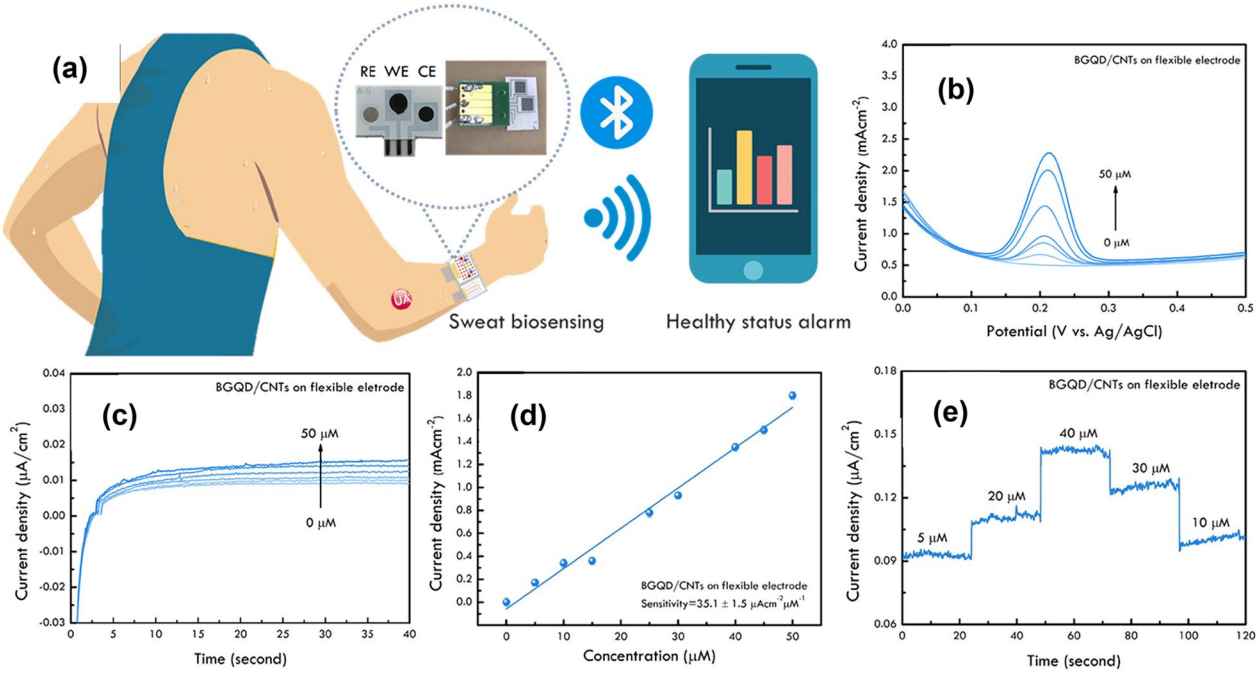

Fig. 3 Wearable biosensor developed with BGQDs/CNTs: **a** Picture of practical use for the flexible electrode constructed from BGQDs/CNTs. **b** DPV curves for the flexible BGQDs/CNTs electrode in the UA concentration range of 0–50 μM. **c** Amperometric responses of a flexible BGQDs/CNTs electrode at an applied potential of 0.2 V. **d** UA calibration curve for flexible BGQDs/CNTs electrode with a linear range of 0–50 μM. **e** Time sequence diagram for the flexible BGQDs/CNTs electrode with the UA level and time (Reproduce with permission from Ref. Wang et al. 2022, Copyright 2022, American Chemical Society)

nanoparticles, and multiwalled carbon nanotubes have recently been reported for use in norepinephrine (Fajardo et al. 2019), and DA (Arumugasamy et al. 2020) sensors.

Simultaneous detection of small molecules is crucial because small molecules with similar oxidation potentials cause the superimposition of electrochemical signals. Chul Lim et al. (2022) reported a novel method for producing GQD-doped poly(3,4-ethylene dioxythiophene) (PEDOT) on a glassy carbon electrode (GCE) using a one-step electro-polymerization process. The GQD-PEDOT composite was used as an effective electrode material for the simultaneous detection of ascorbic acid (AA), DA, and UA. GQD promotes a conformational shift of PEDOT to a quinoid structure, forming oxidized PEDOT. This increases π–π interaction with the aromatic moiety of analytes and intermolecular interaction between PEDOT chains, affording effective electron transfer. Saisree et al. (2022) demonstrated the use of nitrogen-doped GQD (N-GQD) with copper nanocluster (CuNC) composite for the simultaneous electrochemical detection of DA, SER, and nicotine (NIC) with a good peak-to-peak separation (Fig. 4). The impressive performance can be assigned to the synergistic effect of the N-GQD and the CuNC as well as interactions between the sensor and the analytes via ring stacking or the π–π interaction between the aromatic basal planes or heteroatom sites or a combination of all these factors.

GQDs serve as an appropriate substrate for aptamers via π–π stacking interactions, enhancing aptamer absorption on the electrode surface (Mansuriya and Altintas 2020). Therefore, various GQDs-based nanocomposites for electrochemical aptamers or immunosensors have been designed and developed (Mansuriya and Altintas 2019). Savas and Altintas (2019) developed a new, fast, label-free, ultrasensitive, and highly specific immunosensor using GQDs as enzyme mimics in an electrochemical sensor to provide an efficient diagnostic method for *Yersinia enterocolitica*.

Mansuriya and Altintas developed an ultrasensitive enzyme-free electrochemical nano-immunosensor, and SWV technique was used to detect cardiac troponin-I (cTnI) for the early identification of acute myocardial infarction (Mansuriya and Altintas 2021). It is based on a screen-printed gold electrode modified with GQDs and gold nanoparticles (AuNPs). They revealed that GQDs and AuNPs were specifically used as nanozymes and signal-amplifying materials to replace the enzyme systems and enhance the sensitivity of the developed nano-immunosensor.

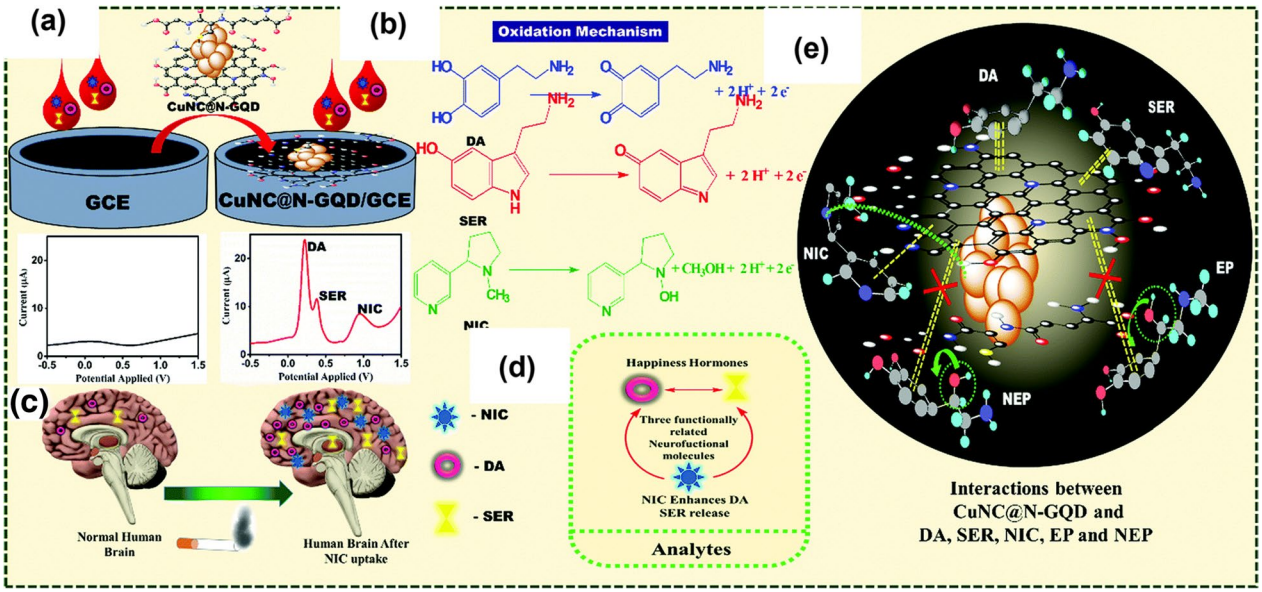

Fig. 4 **a** Schematic showing the modification of GCE with the CuNC@N-GQDs and the resultant enhanced sensing of DA, SER, and NIC; **b** the oxidation mechanisms of DA, SER, and NIC on CuNC@N-GQD/GCE; **c** a diagrammatic representation of the enhanced release of DA and SER in the brain during NIC intake; **d** a flowchart showing the functional correlation between DA, SER, and NIC; and **e** the interactions among CuNC@N-GQDs and the analytes DA, SER, NIC, EP, and NEP based on the structural and functional features (Reproduce with permission from Ref. Saisree et al. 2022, Copyright 2022, Royal Society of Chemistry)

Similarly, Tran et al. (2022) reported the incorporation of N-GQDs and phytohemagglutinin-L (PHA-L) onto screen-printed electrodes for the detection of breast cancer cells (MCF-7) in human serum. According to Mollarasouli et al. (2018), the disposable immune-sensing platform is formed by immobilizing the specific anti-AXL antibody onto amine-functionalized GQDs-modified screen-printed carbon electrodes for the detection of biomarker receptor tyrosine kinase (AXL) in human serum (Fig. 5). The use of amine-functionalized GQDs improved the kinetics of the electron transfer reaction, allowing the attachment of large antibody loadings

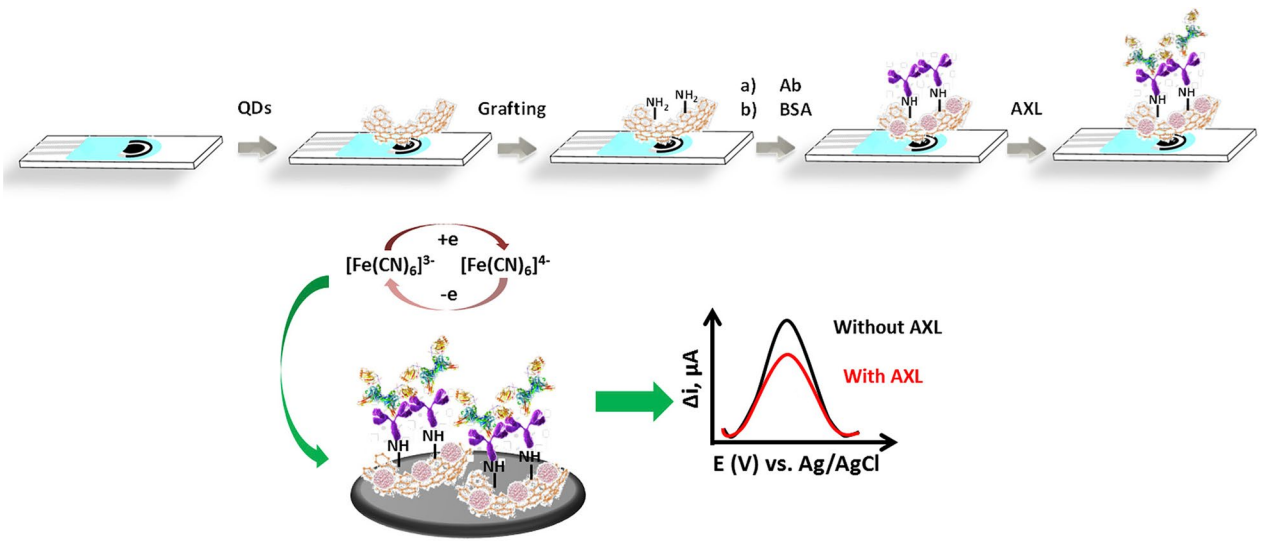

Fig. 5 Schematic of the different steps in constructing a label-free immunosensor for AXL, which involves amine-functionalized GQDs-modified screen-printed carbon electrodes and covalent immobilization of anti-AXL through oxidized sugar chains (Reproduced with permission from Ref. Mollarasouli et al. 2018, Copyright 2018, Elsevier)

owing to in situ electrode functionalization with a high number of amine groups, resulting in a high sensitivity of the immunosensor developed in their work. Gogola et al. (2021) reported an apta-sensor that detects human immunodeficiency virus (HIV) via p24 proteins. In their research, graphene QDs were used to improve the amplification of an electrochemical signal and to help immobilize the p24-HIV aptamer on the device. Furthermore, it was reported that the developed apta-sensor successfully distinguished between positive and negative samples in spiked human serum. Table 1 summarizes some GQDs-based nanocomposites for voltammetric sensors reported recently.

GQDs-based nanocomposites for amperometric sensors

Amperometry is a technique for measuring cell current overtime after a fixed potential has been applied. It can be used in response to successive addition of analytes, as well as electroactive substances that demonstrate redox current as a function of time (Xu et al. 2017).

Tashkhourian et al. (2018) used GQD to construct a simply modified carbon paste electrode (CPE) with chitosan (CS) as a stabilizing agent to develop a new electrochemical sensor. The objective of this study was to develop an amperometric sensor for the detection of epinephrine. Amperometry analysis revealed a linear range of 0.36–380 µM, with no interference from typical interfering substances (AA, DA, and UA). An amperometric hydrogen peroxide (H_2O_2) sensor was developed by Xu et al. (2018) using carbon fiber with dual nanoenzyme, i.e., AuPd alloy nanoparticles (AuPd-ANPs) decorated GQDs assembly (Fig. 6). In this system, the authors suggested the AuPd-ANPs/GQDs/ACF microelectrode displays good sensing performances and can be used for real-time tracking of H_2O_2 released from different types of living human breast cancer cells and in situ H_2O_2 detection in clinical breast cancer tissue. Thirumalai

Table 1 Some of the GQD-based nanocomposites for voltammetric sensors

Electrode material	GQD preparation method (precursor)	Target analyte	Electroanalytical technique	Linear range	LOD	References
BGQD/CNTs[a]	Hydrothermal (citric acid)	UA	Differential pulse voltammetry (DPV)	5.0×10^{-6}–5.0×10^{-5} M	9.9×10^{-7} M	Wang et al. (2022)
MIP/GQDs/2D-hBN/GCE	Thermal deoxidization (graphene oxide)	SER	DPV	1.0×10^{-12}–1.0×10^{-8} M	2.0×10^{-13} M	Yola and Atar (2018)
TC–GQD	Hydrothermal (espresso coffee wastes)	DA	DPV	1.0×10^{-6}–5.0×10^{-4} M	2.2×10^{-7} M	Ahmadi et al. (2020)
AuNPs/GQDs/GCE	Pyrolysis (citric acid)	Norepinephrine (NE)	Square-wave stripping voltammetry	5.0×10^{-7}–7.5×10^{-6} M	1.5×10^{-7} M	Fajardo et al. (2019)
GQDs@MWCNTs/GCE	Pyrolysis (glucose)	DA	DPV	2.5×10^{-7}–2.5×10^{-4} M	9.5×10^{-8} M	Arumugasamy et al. (2020)
PEDOT-GQD/GCE	Electro polymerization (carbon nanofibers)	AA, DA, and UA	DPV	AA: 3.0×10^{-5}–1.0×10^{-3} M DA: 5.0×10^{-7}–4.0×10^{-5} M UA: 1.0×10^{-6}–1.0×10^{-4} M	4.1×10^{-6} M 1.2×10^{-7} M 1.8×10^{-7} M	Chul Lim et al. (2022)
CuNC@ N-GQD/GCE	Hydrothermal (polyaniline)	DA, SER, and NIC	DPV	DA: 1.0×10^{-12}–1.0×10^{-6} M SER: 1.0×10^{-9}–1.0×10^{-6} M NIC: 1.0×10^{-11}–1.0×10^{-6} M	1.0×10^{-12} M 1.0×10^{-9} M 1.0×10^{-11} M	Saisree et al. (2022)
Anti-cTnI/AuNPs@GQDs/SPGE	Commercial GQD from Sigma	Cardiac troponin-I	Square-wave voltammetry	1.0–1000 pg mL^{-1}	0.10 pg mL^{-1}	Mansuriya and Altintas (2021)
N-GQDs/PHA-L	Microwave-assisted hydrothermal (passion fruit juice)	Human breast cancer cells (MCF-7)	Linear sweep voltammetry	5–20×10^{6} cells mL^{-1}	1.0 cell mL^{-1}	Tran et al. (2022)
Anti-AXL-fGQDs/SPCE	Pyrolysis (citric acid)	AXL receptor tyrosine kinase	DPV	1.7 pg mL^{-1}–1.0 ng mL^{-1}	0.5 pg mL^{-1}	Mollarasouli et al. (2018)
GQD-SPE/aptamer	Pyrolysis (citric acid)	p24-HIV	Cyclic voltammetry	0.93 ng mL^{-1}–93 µg mL^{-1}	51.0 pg mL^{-1}	Gogola et al. (2021)

[a] *BGQD* boron-doped graphene quantum dots, *CNTs* carbon nanotubes, *TC* titania–ceria, *AuNPs* gold nanoparticles, *MWCNTs* multiwalled carbon nanotubes, *PEDOT* poly(3,4-ethylene dioxythiophene), *CuNC* copper nanocluster, *N-GQD* nitrogen-doped graphene quantum dots, *GCE* glassy carbon electrode, *MIP* molecularly imprinted polymer, *Anti-cTnI* anti-cardiac troponin-I, *SPGE* screen-printed gold electrode, *PHA-L* phytohemagglutinin-L, *Anti-AXL* anti-receptor tyrosine kinase, *fGQDs* amine-functionalized graphene quantum dots, *SPCE* screen-printed carbon electrode

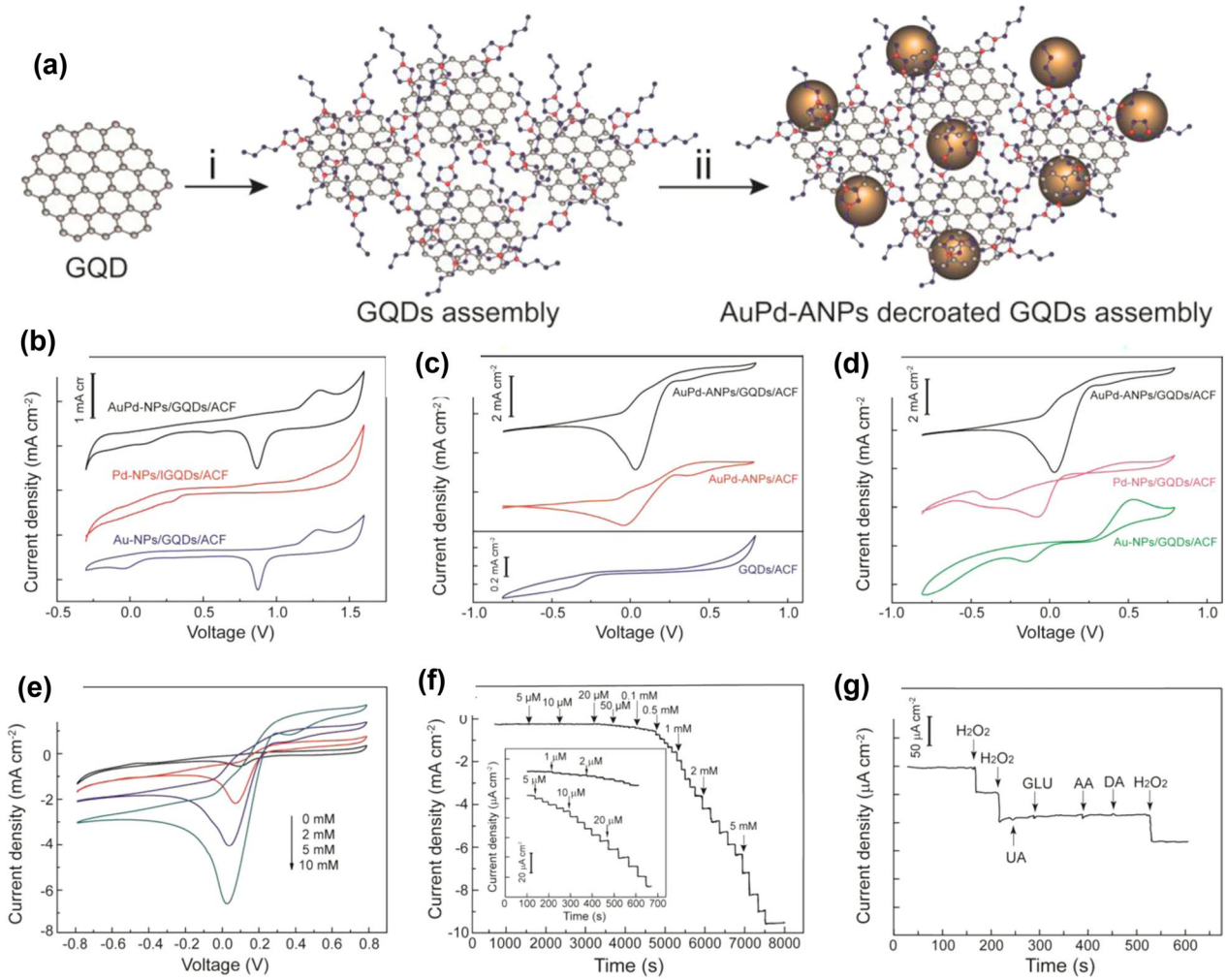

Fig. 6 **a** Schematic representation of GQDs assembly and AuPd-ANPs decorated GQDs assembly formation. Step 1: Electrodeposition of GQDs on ACF with [BMIM]OTF as the electrolyte to form a close-pack GQDs assembly; Step 2: Electrodeposition of AuPd-ANPs on GQDs on ACF. **b** CV curves of AuPd-ANPs/GQDs/ACF, Au-NPs/GQDs/ACF, and Pd-NPs/GQDs/ACF microelectrodes in 0.5 M H_2SO_4. Scan rate: 50 mV s^{-1}. **c** CV curves of AuPd-ANPs/GQDs/ACF, AuPd-ANPs/ACF, and GQDs/ACF microelectrodes in 0.1 M PBS solution containing 5 mM H_2O_2. Scan rate: 50 mV s^{-1}. **d** CV curves of AuPd-ANPs/GQDs/ACF, Pd-NPs/GQDs/ACF, and Au-NPs/GQDs/ACF microelectrodes in 0.1 M PBS solution containing 5 mM H_2O_2. Scan rate: 50 mV s^{-1}. **e** CV curves of AuPd-ANPs/GQDs/ACF electrode in 0.1 M PBS solution containing 0, 2, 5, and 10 mM H_2O_2. Scan rate: 50 mV s^{-1}. **f** Typical amperometric response of AuPd-ANPs/GQDs/ACF microelectrode to successive addition of different H_2O_2 concentrations into 0.1 M PBS solution under stirring. Inset of **f** is the amperometric response of AuPd-ANPs/GQDs/ACF electrodes at low concentrations. Applied potential: 0.05 V. **g** Amperometric response of AuPd-ANPs/GQDs/ACF to successive addition of 0.1 mM H_2O_2 and 0.1 mM UA, GLU, AA, and DA in 0.1 M PBS. Applied potential: 0.05 V. (Reproduced with permission from Ref. Xu et al. 2018, Copyright 2018, Elsevier)

et al. (2020) described a simple method for developing reagent-free amperometric pyruvate biosensors based on enzyme nanoparticles (EnNPs). EnNPs were produced by crosslinking pyruvate oxidase with GQDs. Prussian blue, a biocompatible coordination polymer, was used to modify screen-printed carbon electrodes (SPCEs) prior to EnNP immobilization. According to the authors, the developed pyruvate biosensor has high sensitivity, selectivity, and reproducibility. As a result, it could be a promising candidate for new enzyme-based biosensors, specifically for pyruvate detection.

GQDs-based nanocomposites for impedimetric sensors

Electrochemical impedance spectroscopy is a technique that can be used to monitor changes in the interfacial properties of an electrode surface. This is advantageous because it does not require any additional signal-generating labels, and it is not destructive. Additionally, EIS

is not affected by the analytes and can be used to study them without any interference (Magar et al. 2021).

Nxele and Nyokong (2021) have developed an impedimetric sensor that can be used to detect prostate-specific antigens (PSA). They have combined a PSA-specific aptamer and a cobalt phthalocyanine with GQDs, N-GQDs, and graphitic carbon nitride quantum dots (gCNQDs) to study the effects of the type of QDs on the sensor's electrocatalytic ability. They found that the N-GQDs-based electrode had the lowest LOD compared to the other sensors. The high performance of N-GQDs was predicted because they are known to perform better in electrocatalysis than GQDs owing to the incorporation of nitrogen atoms into the graphitic structure. Similarly, conductive polypyrrole with sulfur/nitrogen-doped GQDs and cobalt phthalocyanine composite can be used for impedimetric human epidermal growth factor receptor 2 (HER2) detection (Centane and Nyokong 2021). According to the authors, the study observed that developed immunosensors are very sensitive, with a detection limit of 0.00141 ng/mL. This makes them suitable for the determination of HER2 in serum samples with high accuracy and reproducibility. Ganganboina et al. (2021) reported that sulfur-doped GQDs (S-GQDs) are deposited onto gold nanoparticles, which are then decorated with carbon nanospheres (Fig. 7). The S-GQDs@Au-CNS nanocomposite is then used as a dual-function probe for enhancing electrochemical activity and conjugating the angiopep-2 protein for glioma cell detection. Table 2 summarizes some GQDs-based nanocomposites for amperometric and impedimetric sensors reported recently.

Optical sensors

The excellent optical and fluorescence properties of GQDs are the main factors that GQDs are often combined with other materials as optical sensors. Good biocompatibility properties and oxygen-rich functional groups of GQDs are becoming advantages of GQDs to be used in biosensing applications which is different from other quantum dot-based materials that suffer from toxicity issues. Several studies are reported the good performance of GQDs as a composite material in optical sensors, such as surface-enhanced Raman scattering and fluorescence sensors.

GQDs-based nanocomposites for SERS sensors

Raman spectroscopy is an important tool for characterization and biosensing as it provides a chemical fingerprint for molecular identification (Koh et al. 2021; Serebrennikova et al. 2021). Long-term research has been conducted on developing substrates for increasing the Raman signal (Cheng et al. 2012). Several nanostructured materials, known as SERS substrates, have been developed to provide a highly sensitive vibrational technique for identifying trace analytes. The detection of multiplex targets was investigated using their characteristic vibrational fingerprints (Jung et al. 2019; Linh et al. 2021; Plou et al. 2021). Noble and transition metals have been used as substrates for SERS owing to their plasmonic properties (Linh et al. 2019a; b). However, developing novel SERS substrates is still required to meet rigorous requirements such as cost, stability, reliability, and biocompatibility (Cheng et al. 2012).

As a "miracle material" with a crystal package of carbon atoms, graphene-based materials exhibit interesting Raman scattering properties, which are promising in SERS applications owing to excellent adsorption and chemical properties (Bali Prasad et al. 2017; Cheng et al. 2012; Mary and Mary 2021). GQDs comprising graphene sheets with sizes < 10 nm have attracted enormous attention owing to high optical absorptivity, excellent chemical stability, biocompatibility, and efficient charge transfer (CT) properties suitable for a SERS substrate (Zheng et al. 2015). Plasmonic metals such as Au and Ag (Fig. 8) show a considerably good SERS sensitivity when the particle size is > 30 nm (Jin et al. 2022). However, it would be difficult to use plasmonic metal nanostructure for biological applications such as intracellular analysis that requires a small size to enter cells via endocytosis (Jin et al. 2022; Wu et al. 2019). The small-sized plasmonic nanostructure frequently exhibits poor SERS activity owing to reduced localized surface plasmon resonance (Pustovit and Shahbazyan 2006). According to Butler et al. (2015), the small size of the plasmonic nanostructure also generates high toxicity resulting from biological damage. This challenge restricts plasmonic metal nanostructures to be used in the biological field (Jin et al. 2022).

The dense GQDs can exhibit noticeable SERS sensitivities through enhancements of the electromagnetic mechanism (EM) and chemical mechanism (CM) (Jin et al. 2022; Liu et al. 2018a). The rational assembly of GQDs in nanoarchitecture could effectively adsorb target molecules and harvest collective Raman signals (Cheng et al. 2012). However, Das et al. (2020) reported no clarity on the individual contributions of GQDs on SERS performance. Classifying the type of interaction, CT, and individual contributions in SERS is still challenging.

Several studies have found that combining GQDs and metal materials provides high SERS signals for identifying target molecules owing to their optical and electronic properties (Cheng et al. 2012; Mary and Mary 2021). As shown in Fig. 9, GQDs contribute to higher SERS activity than bare metal. The high SERS activity of this combination is due to the synergistic contribution between noble

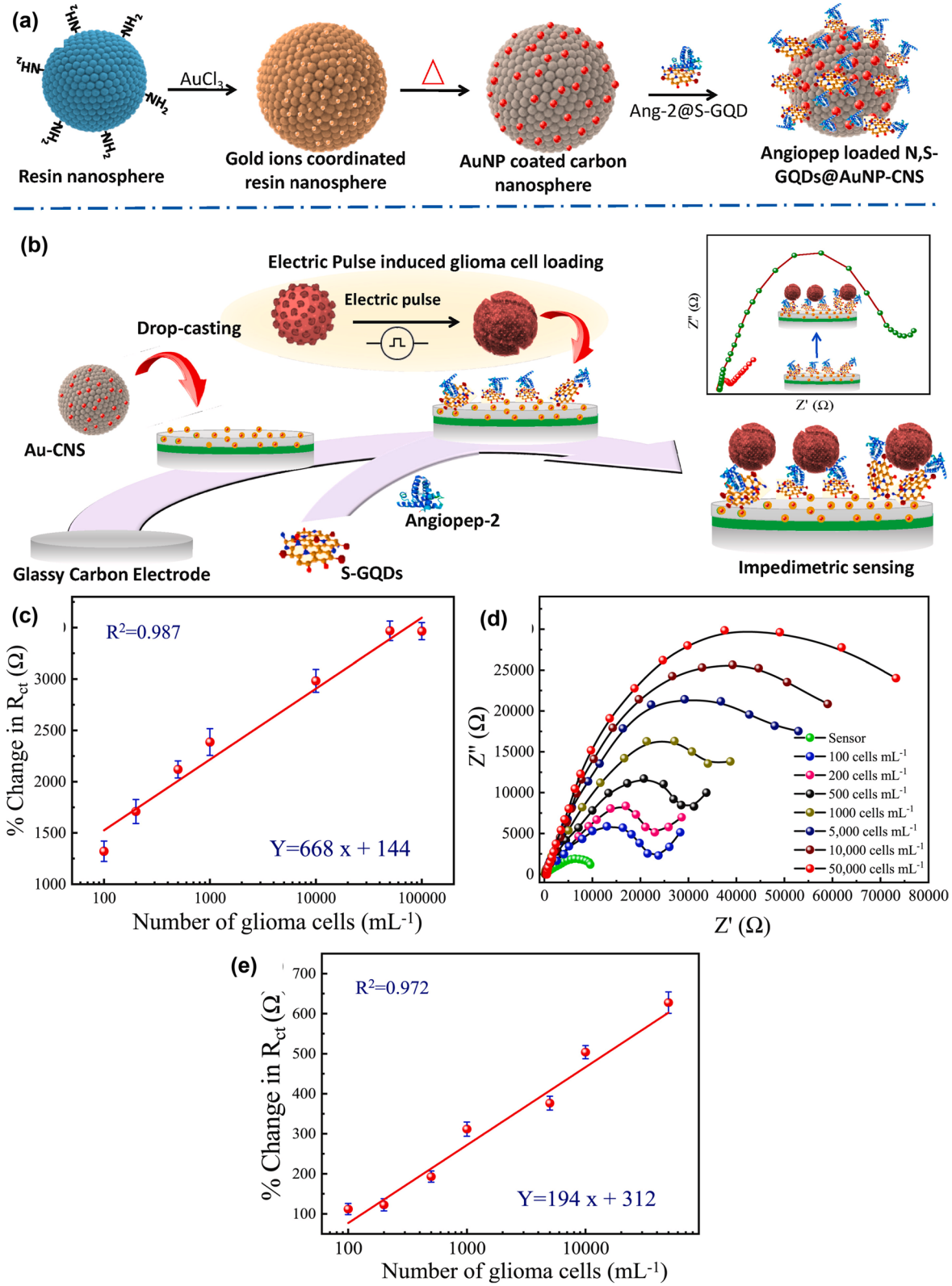

Fig. 7 **a** Illustration of the synthesis and fabrication of GCE||Au–CNS@S-GQD/Ang-2 biosensor, **b** pulse-induced electrochemical detection of glioma cells, **c** calibration line obtained from change in R_{ct} versus glioma cells concentration, **d** Nyquist plot of GCE||CNS–Au@S-GQDs/Ang-2 sensor at different concentrations of glioma cells in human serum, and **e** calibration line obtained from the change in R_{ct} versus glioma cells concentration (Reproduced with permission from Ref. Ganganboina et al. 2021, Copyright 2021, Elsevier)

Table 2 Some of the GQDs-based nanocomposites for amperometric and impedimetric sensors

Electrode material	GQD preparation method (precursor)	Target analyte	Electroanalytical technique	Linear range	LOD	References
GQD-CS/CPE	Hydrothermal (citric acid)	Epinephrine (EP)	Amperometry	3.6×10^{-7}–3.8×10^{-4} M	3.0×10^{-10} M	Tashkhourian et al. (2018)
AuPd-ANPs/GQDs/ACF	Pyrolysis (citric acid)	Hydrogen peroxide (H_2O_2)	Amperometry	1.0×10^{-6}–1.8×10^{-2} M	5.0×10^{-7} M	Xu et al. (2018)
PoxBNP/PB/SPCE	Commercial GQD from Sigma	Pyruvate	Amperometry	1.0×10^{-5}–7.5×10^{-4} M	9.1×10^{-7} M	Thirumalai et al. (2020)
GCE-N-GQDs-CoPc-Aptamer	Hydrothermal (citric acid)	Prostate-specific aptamer (PSA)	Impedimetric	0.034–0.057 ng mL^{-1}	0.044 ng mL^{-1}	Nxele and Nyokong (2021)
GCE/PPy@SNGQDs/CoPc	Hydrothermal (citric acid)	Human epidermal growth factor receptor 2	Impedimetric	1.0–10 ng mL^{-1}	1.41 pg mL^{-1}	Centane and Nyokong (2021)
GCE‖CNS-AuNPs@S-GQDs/Ang-2	Pyrolysis (citric acid)	Glioma cell	Impedimetric	100–100,000 cells mL^{-1}	40 cells mL^{-1}	Ganganboina et al. (2021)

CS chitosan, *CPE* carbon paste electrode, *AuPd-ANPs* AuPd alloy nanoparticles, *ACF* activated carbon fiber, *PoxBNP* PoxB with GQD, *PB* Prussian blue, *SPCE* screen-printed carbon electrodes, *SPE* screen-printed electrodes, *p24-HIV* p24-human immunodeficiency virus, *N-GQDs* nitrogen-doped graphene quantum dots, *CoPc* Co(II) phthalocyanine, *Anti-AXL* anti-AXL receptor tyrosine kinase, *fGQDs* amine-functionalized graphene quantum dots, *SPCE* screen-printed carbon electrodes, *PHA-L* phytohemagglutinin-L, *LSV* linear sweep voltammetry, *BSA* bovine serum albumin, *Anti-OTA* anti-ochratoxin A, ZrO_2 zirconium dioxide, *ITO* indium tin oxide, *Anti-cTnI* anti-cardiac troponin-I, *AuNPs* gold nanoparticles, *SPGE* screen-printed gold electrode, *PPy* polypyrrole, *SNGQDs* sulfur/nitrogen-doped graphene quantum dots, *CoPc* cobalt phthalocyanine, *CNS-AuNPs* gold nanoparticles decorated carbon nanospheres, *S-GQDs* sulfur-doped graphene quantum dots, *Ang-2* angiopep-2

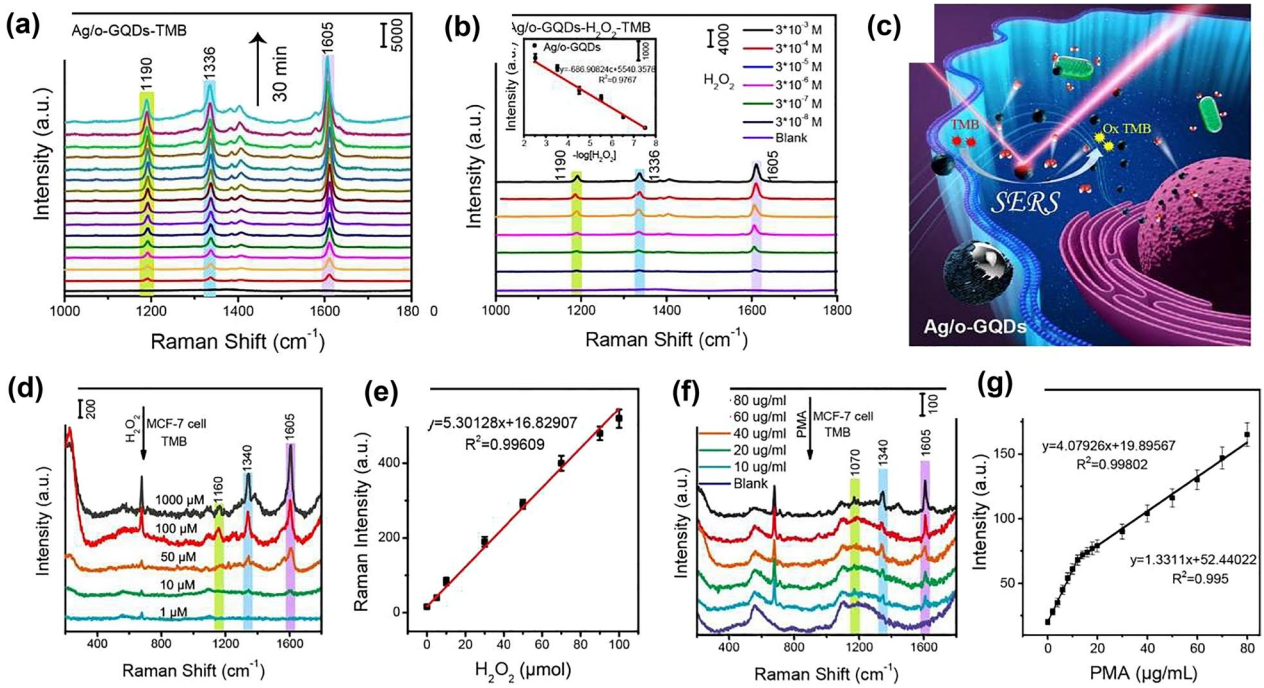

Fig. 8 **a** SERS spectra for the oxTMB catalyzed by Ag/o-GQDs in the presence of H_2O_2 (3 mM). The time interval between successive curves is 2 min. **b** SERS spectra for the oxTMB catalyzed by Ag/o-GQDs with the H_2O_2 concentration range (3–30 nM). Inset: Quantitative analysis plot of oxTMB at 1605 cm^{-1} with different H_2O_2 concentrations, Error bars = SD, $n = 3$. **c** Schematic diagram of the SERS-active Ag/o-GQDs nanozyme-triggered in situ catalytic oxTMB for cancer cell H_2O_2 detention and ROS-mediated therapy. **d** SERS spectra for the oxidation of TMB catalyzed by Ag/o-GQDs in MCF-7 cells treated with various concentrations of the exogenous introduction of H_2O_2 (1–1000 μM). **e** Plots of the SERS response of oxTMB at 1605 cm^{-1} catalyzed by Ag/o-GQDs in MCF-7 cells treated with various concentrations of H_2O_2. **f** SERS spectra for the oxTMB catalyzed by Ag/o-GQDs in MCF-7 cells treated with the various concentrations of PMA (0–80 μg/mL). **g** Plots of the SERS response of oxTMB at 1605 cm^{-1} catalyzed by Ag/o-GQDs with H_2O_2 release from MCF-7 cells upon the stimulation of PMA (Reproduced with permission from Ref. Jin et al. 2022, Copyright 2022, Elsevier)

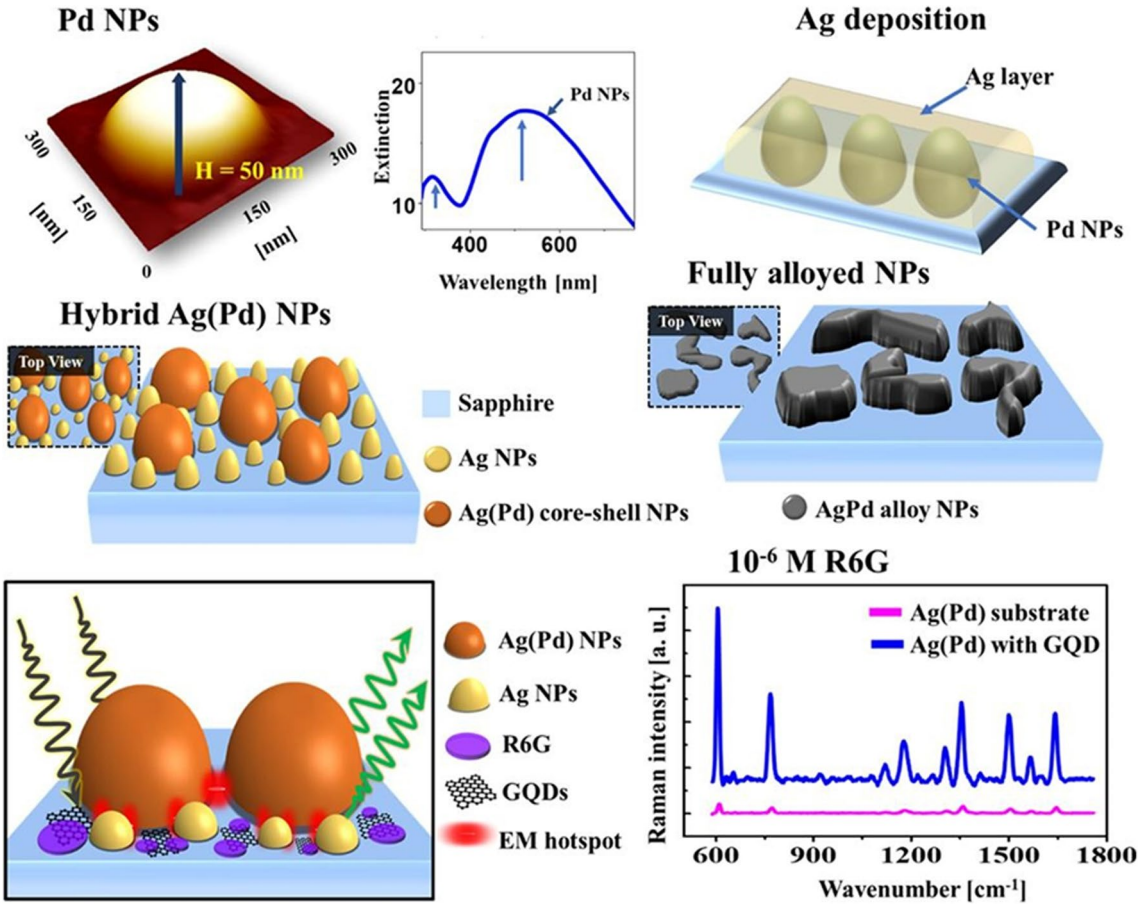

Fig. 9 The effect of GQDs on metal nanocomposite for SERS substrate (Reproduced with permission from Ref. Pandit et al. 2021, Copyright 2021, Elsevier)

metals and GQDs. According to Anithaa et al. (2017) and Motahari et al. (2012), GQDs can absorb analyte molecules via π–π stacking, electrostatic interactions, and hydrophilic interactions. The interactions between adsorbed molecules and GQDs induce the CT process, which provides extra Raman enhancement during measurement, often called CM enhancement (Fan et al. 2012; Pandit et al. 2021). Liu et al. (2018a) explained that π–π stacking is not the only factor that affects the SERS signal in graphitic material. It can also be ascribed to GQDs being an interfacial layer between the noble metal and target molecules, inducing the CT process. Meanwhile, the SERS activity of noble metals is mainly attributed to EM enhancement owing to their localized surface plasmon resonance (LSPR) (Langer et al. 2020; Valley et al. 2013). For instance, Fei et al. (2017) reported that the nanoflower structure of noble metal exhibits a strong LSPR, which generates a strong electromagnetic field (called "hot spots") on the tip of the petal and within a small gap between the petal and the particle. Even though GQDs often contribute through CM enhancement, some studies have reported that GQDs also participate in EM enhancement. Pandit et al. (2021) and Ge et al. (2016) reported that GQDs can create plasmonic hot spots between metal nanoparticles. Consequently, high-density small gaps were generated, and the Raman signal could be intensified through EM enhancement. However, the amount of GQDs is important in generating nanogap between the particles, where a high concentration of GQDs can reduce the SERS activity of metal-GQDs owing to GQDs blocking hot spot sites, preventing analyte molecules from adsorbing on the surface (Pandit et al. 2021).

Recently, GQDs nanocomposite-based studies for Raman sensors, especially SERS, have substantially increased. Several biofield areas have been explored, including biochemical analytes, cancer cells, and bacterial protein, as shown in Table 3. The unique physicochemical properties of GQDs are promising to support noble metals or metal oxides as SERS substrates (Fan et al. 2018). The construction of metal–GQDs nanocomposite may endow them with synergistically improved

Table 3 Some examples of GQDs-based nanocomposites for SERS sensor

Material	GQD preparation method	Target analyte	Raman technique	Linear range (M)	LOD (M)	EF	References
Ag/o-GQDs (colloidal probe)	Nanocutting method (graphite powder)	H_2O_2	SERS	$0–9\times10^{-5}$	3.17×10^{-6}	2.39×10^{6}	Jin et al. (2022)
MPBA/4-NBT@Au–N-GQD (colloidal probe)	Hydrothermal treatment (CTAB)	L02 cell, HeLa cell, and MCF-7 cell	SERS	–	–	2.01×10^{6}	Miao et al. (2019)
GQD–Mn_3O_4 (colloidal probe)	Nanocutting method (MWCNTs)	7702, HepG-2, and HeLa cells	SERS	–	–	2.06×10^{4}	Lan et al. (2017)
MagPlas NP–GQD (solid substrate)	Chemical oxidation (carbon fiber)	CFP-10	SERS immunoassay	$1\times10^{-12}–1\times10^{-6}$	5×10^{-14}	–	Zou et al. (2015)

o-GQDs oxidized graphene quantum dots, *N-GQDs* nitrogen-doped graphene quantum dots, *MPBA* 4-mercaptophenylboronic acid, *4-NBT* 4-nitrobenzene-thiol, *CTAB* cetyltrimethylammonium bromide, *MWCNTs* multiwalled carbon nanotubes, *MagPlas NPs* magneto plasmonic nanoparticles, *L02 cell* human liver cell, *HeLa cell* immortal human cell, *MCF-7 cell* human breast cancer cell, *HepG-2 cell* human liver cancer cell, *CFP-10* antigen from mycobacterium tuberculosis

catalytic activity for catalyzing peroxidase (POD). Jin et al. (2022) reported that the efficient POD-like catalytic activity and excellent SERS sensitivity of Ag/oxidized GQDs (Ag/o-GQDs) make them an ideal platform for in situ SERS monitoring of the nanozyme-catalyzed reaction. The SERS activity came from EM enhancement of noble metal and CT resonance between Ag/o-GQDs and oxidized 3,3′,5,5′-tetramethylbenzidine (oxTMB). The small size of GQDs provides an effective platform for intracellular analysis with in situ SERS monitoring, which noble metals could not accomplish owing to the lack of SERS activity in small size (Pustovit and Shahbazyan 2006). A similar study about POD monitoring via SERS was reported by Zhao et al. (2017) regarding the oxidation of TMB in the presence of H_2O_2. They showed that metal/GQDs could be used as a nanocatalyst for the oxidation of TMB and as an efficient SERS substrate for monitoring the intensity change of TMB.

Metal–GQDs can be used to develop Raman probes because of their high Raman enhancements, substantial monodispersity, good signal uniformity, and long-term stability (Miao et al. 2019). Au–N–GQDs nanoparticles were commodified with 4-mercapto phenylboronic acid (MPBA) and 4-nitrobenzene-thiol (4-NBT) via Au–S bonding, where MPBA and 4-NBT serve as the glycan recognition unit and Raman reporter, respectively. At a physiological pH of 7.4, MPBA could specifically bind to the C-8,9 diol of glycans via strong esterification. Consequently, after treating the cells with the Au–N–GQDs probes, the glycan expression on the cell membrane can be analyzed.

Lan et al. (2017) also reported the good performance of GQDs-based nanocomposite material (GQDs–Mn_3O_4) for cancer cell detection**.** This material can reveal a characteristic of HeLa cells, indicating that the combination of metal oxide and GQDs can be used as an active substrate for Raman substrates. Zou et al. (2015) reported that GQDs modified with antibodies could capture antigens such as CFP-10, which is secreted from *Mycobacterium tuberculosis*. GQDs on the immunoassay protocol act as dual mode nanoprobes to enhance SERS and fluorescence signals.

GQDs-based nanocomposites for fluorescence sensors

Biofluids such as urea, serum, saliva, and blood are complex body fluids with dynamic biomatrix, including biomolecules, electrolytes, waste products, and various pathogens, that contain information for diagnosing and monitoring diseases (Tagit and Hildebrandt 2017). Fluorescence sensing or fluorescence labeling is the most commonly used technique for metabolite detection owing to its simplicity, non-destructiveness, rapid signal generation and detection, and diversity.

GQDs-based nanocomposites have recently been used to develop various photoluminescence sensors, including fluorescence sensors, as alternatives to conventional fluorophores, which suffer from photobleaching (Salehnia et al. 2017).

Table 4 presents several GQDs-based nanocomposite studies that have investigated various metabolite fields. Most studies used the fluorescence "turn off–on" technique depending on the interaction between an analyte and receptor molecules, causing quenching or fluorescence recovery (Gupta and Kumar 2016). The present technique has realized the sensitive and simple determination of active biological molecules with excellent selectivity. For instance, Huang et al. (2015) introduced Cr(VI) on GQDs as a quencher for the detection of AA, where the presence of Cr(VI) in the system can quench the fluorescence of GQDs owing to the overlapping of the absorption spectra of Cr(VI) and both the excitation and emission spectra of GQDs. Thus, Cr(VI)

Table 4 Some examples of GQDs-based nanocomposites for fluorescence metabolite sensing

Material	GQD preparation method	Target analyte	Fluorescence technique	Linear range	LOD	References
LDH–GQDs	Hydrothermal treatment (citric acid)	Ascorbic acid (AA)	Fluorescence "turn off–on"	5×10^{-6}–3×10^{-4} M	1.72×10^{-6} M	Shi et al. (2021)
N-GQDs@V_2O_5	Hydrothermal treatment (citric acid and urea)	Cysteine	Fluorescence "turn off–on"	1×10^{-7}–1.25×10^{-4} M	5×10^{-8} M	Ganganboina et al. (2018)
MIPs@PIn-BAc/GQDs	Pyrolysis (citric acid)	Dopamine (DA)	Fluorescence quenching	5×10^{-9}–1.2×10^{-6} M	2.5×10^{-9} M	Zhou et al. (2017)
GQDs@AgNPs	Oxidative cutting (GO powder)	H_2O_2	Fluorescence quenching	5×10^{-7}–1×10^{-4} M	5×10^{-7} M	Mehata and Biswas (2021)
GLY-GQDs-Ce (IV)	Pyrolysis	Ascorbic acid (AA)	Fluorescence "turn off–on"	3×10^{-8}–1.67×10^{-5} M	2.5×10^{-8} M	Liu et al. (2017a)
GQDs@GSH	Pyrolysis (citric acid)	Acid phosphatase (ACP)	Fluorescence "turn off–on"	1×10^{-1}–9 mU mL^{-1}	2.7×10^{-2} mU mL^{-1}	Qu et al. (2019)
Arg–GQDs	Hydrothermal treatment (citric acid)	Thiamine	Fluorescence "turn off–on"	1×10^{-7}–8×10^{-6} M	5.3×10^{-8} M	Nemati et al. (2018)
GQDs/AuNCs/Fe^{2+}	Pyrolysis (trisodium citrate)	Glucose	Ratiometric fluorescence probe	1×10^{-6}–1.5×10^{-5} M	1.8×10^{-7} M	Hong et al. (2020)

LDH layered double hydroxides, *N-GQDs* nitrogen-doped graphene quantum dots, *MIP* molecular imprinting polymers, *Pin-BAc* poly(indolylboronic acid), *GLY-GQDs* glycine-functionalized graphene quantum dots, *GSH* glutathione, *Arg* arginine

absorbs the emission light from GQDs which causes the "turn off" of fluorescence. Similar studies have reported that other metal ions such as Hg^{2+}, Fe^{3+}, and Cu^{2+} act as quenchers in GQDs systems (Chakraborti et al. 2013; Ju and Chen 2014; Wang et al. 2014). Liu et al. (2013) reported similar phenomena in which the strong fluorescence of the GQDs@Glutathione (GQDs@GSH) was quenched in the presence of Fe^{3+}. The quenching effect has been primarily caused by the effective electron transfer from GQDs@GSH to Fe^{3+}. However, the affinity between metal ions and systems should be considered to determine the effective metal ions to quench the fluorescence emission of GQDs (Wang et al. 2014). Meanwhile, the presence of AA in the system, which acts as a reducing agent, causes Cr(VI) reduction to lower-valent Cr species that do not affect the fluorescence intensity of GQDs. This phenomenon is often called fluorescence "turn on" for analyte detection (Huang et al. 2015). A similar study was reported by Shi et al. (2021) to detect AA through the fluorescence "turn off–on" mechanism, where Fe^{3+} was used as a quencher, as shown in Fig. 10a. AA in the system reduced Fe^{3+} into Fe^{2+} and restored the fluorescence of layered double hydrochloride–GQDs (LDH–GQDs). It can be seen that LDH–GQDs fluorescence emission intensity increases with increasing concentration of AA, as shown in Fig. 10b, c. Similar to metal ions that quench GQDs-based systems, the fluorescence recovery of GQDs also depends on the structure of the metabolite. Figure 10d shows that several metabolites, such as glutathione, glycine, and serine, could not restore the fluorescence of LDH–GQDs as it depends on the affinity between metabolites and receptors. For instance, Li et al. (2015) detected cysteine through the "turn on–off" mechanism, where Hg^{2+} works as an effective quencher to quench the emission of GQDs via CT. The fluorescence of the GQDs was restored by cysteine because it reacted with Hg^{2+}.

Using GQDs as a fluorescent component in metal oxide has proven to be an effective strategy for constructing integrated quenchers on fluorescence "turn off–on" systems to enhance the selectivity and sensitivity of fluorescent sensors (Wolfbeis 2015). For instance, introducing GQDs on 2D materials such as MnO_2 and MoS_2 nanosheets induces a reaction between 2D materials and the surface functional groups of GQDs, causing fluorescence quenching or reduction (Chen et al. 2015). Ganganboina et al. (2018) also reported 2D V_2O_5 on N-GQDs systems, where V_2O_5 exhibits excellent redox activity and the ability to quench the fluorescence of N-GQDs. Notably, V_2O_5 has a strong affinity for N-GQDs owing to electrostatic interactions, which contribute to fluorescence quenching (Song et al. 2015). The presence of cysteine in the systems causes V_2O_5 to reduce into V^{4+} and N-GQDs to release from the N-GQDs@V_2O_5, resulting in the fluorescence intensity being restored (Ganganboina et al. 2018).

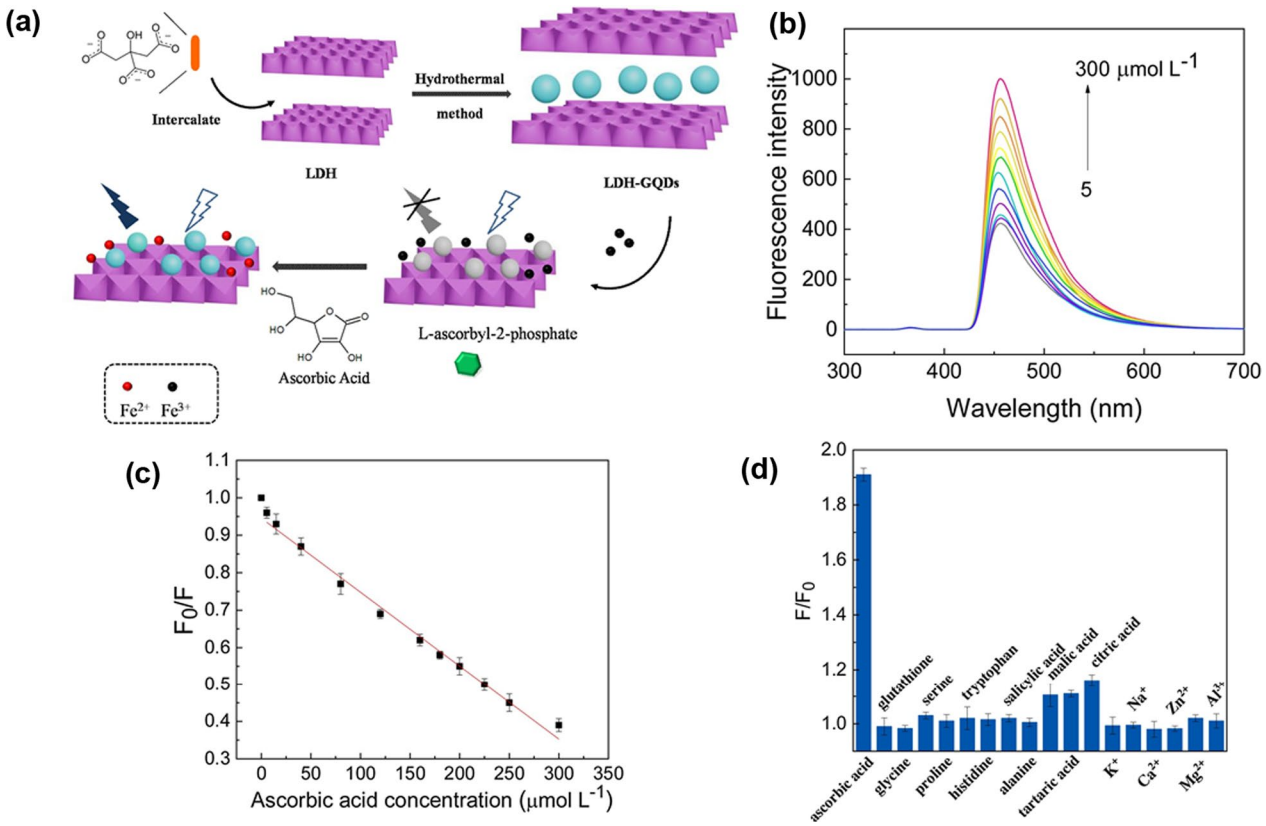

Fig. 10 **a** Procedure and mechanism of LDH–GQDs fluorescence probe for detecting ascorbic acid, **b** fluorescence spectra of LDH–GQDs with different ascorbic acid concentration, **c** Stern–Volmer relationship between F_0/F and ascorbic acid concentration, **d** selectivity performance of LDH–GQDs in ascorbic acid detection (Reproduced with permission from Ref. Shi et al. 2021, Copyright 2021, Elsevier)

The small particle size of GQDs is advantageous in developing fluorescent probes that can distribute in the cytoplasm of the cell and the nuclei (Hong et al. 2018). In plasmonic-enhanced fluorescence, GQDs also can overcome the short lifetime of LSPR which becomes a problem in small particle sizes of plasmonic material (Jin et al. 2022; Lu et al. 2018). In the small size, GQDs also showed a high photostability against photobleaching, which is mainly a problem in the case of organic dyes and semiconductor QDs (Hong et al. 2018).

Several studies have shown the effective role of GQDs-based nanocomposite in cellular fluorescence analysis, as summarized in Table 5. For instance, Asghari and Mahmoudifard (2023) used hyaluronic acid (HA)-functionalized GQDs to detect captured cancer cells on the nanofibrous membrane (NFM) through the change in fluorescence intensity induced by surface charge interaction. Tang et al. (2021) introduced N-GQDs as a fluorescent probe on MoS_2 to overcome biocompatibility issues for the intracellular detection of GSH. The combination between MoS_2 and N-GQDs shows a photo-catalyst ability to produce oxygen radicals for GSH detection, playing an important role in pathological and biological processes through redox reactions (Tang et al. 2021; Zhang et al. 2015b). "Turn-on" fluorescence biosensors based on GQDs and MoS_2 nanosheets were demonstrated for rapid and sensitive detection of epithelial cell adhesion molecule (EpCAM), which is known as a biomarker for diagnosing and prognosis of cancer (Cui et al. 2019), (Shi et al. 2017). The presence of EpCAM on the surface of the circulating tumor cells promotes the separation process of aptamer@Fe_3O_4@GQD from $MoS_{2,}$ resulting in fluorescence recovery and becoming an indicator for EpCAM detection.

The introduction of GQDs as a fluorescent probe on plasmonic materials is an effective strategy for cellular detection, especially in constructing fluorescence "turn off–on" systems (Pei et al. 2015). The LSPR absorption of plasmonic materials is suitable for making devices and assays with unparalleled functionalities for highly sensitive target analysis (Chen et al. 2014). Lu et al. (2018) developed GQDs/Ag NPs for sensing alkaline phosphatase (ALP), a glycoprotein enzyme that can catalyze the dephosphorylation process of nucleic acids,

Table 5 Some examples of GQDs-based nanocomposites for fluorescence cellular sensing

Material	GQD preparation method	Target analyte	Fluorescence technique	Linear range	LOD	References
GQDs/Ag NPs	Pyrolysis (citric acid)	Alkaline phosphatase (ALP)	Fluorescence quenching	0–5 U L^{-1}	2×10^{-2} U L^{-1}	Lu et al. (2018)
N-GQDs-MoS_2	Hydrothermal treatment (citric acid and urea)	Glutathione (GSH)	Fluorescence "turn off–on"	4×10^{-4}–4.4×10^{-3} M	2.47×10^{-6} M	Tang et al. (2021)
Aptamer@ Fe_3O_4@ GQD@ MoS_2	Electrolysis (graphite rods)	Epithelial cell adhesion molecule (EpCAM)	Fluorescence "turn off–on"	2×10^{-9}–6.4×10^{-8} M	1.19×10^{-9} M	Cui et al. (2019)
AuNF@GQDs	Pyrolysis ($_L$-glutamic acid)	MicroRNA-34a	Fluorescence resonance energy transfer (FRET)	1.5×10^{-16}–8×10^{-15} M	1×10^{-16} M	Sun et al. (2018)
Nanoceria @ GQD	Pyrolysis (citric acid)	Ochratoxin A (OA)	FRET	1×10^{-8}–2×10^{5} mg mL^{-1}	2.5×10^{-9} mg mL^{-1}	Tian et al. (2018)
Py-MBs–GQDs	Pyrolysis (citric acid)	MicroRNA	FRET	1×10^{-10}–2×10^{-7} M	1×10^{-10} M	Zhang et al. (2015a)
BN–SGQD	Solvothermal	Human immunodeficiency virus (HIV) DNA	FRET	0–2×10^{-8} M	5×10^{-10} M	Li et al. (2017)
GQDs-CuNC	Hydrothermal treatment (citric acid)	Human T cell lymphotropic virus type I (HTLV-I)	Fluorescence	2×10^{-11}–1.2×10^{-8} M	1×10^{-11} M	Chen et al. (2021)
ITO–GQDs–CM–APOE DNA	Pyrolysis (citric acid)	APO*e4* DNA	Dual (fluorescence/amperometry)	2×10^{-8}–4×10^{-7} mg mL^{-1}	2.18×10^{-9} mg mL^{-1}	Mars et al. (2018)

N-GQDs nitrogen-doped graphene quantum dots, *AuNF* gold nanoflower, *Py-MBs* pyrene-functionalized molecular beacon probes, *BN-SGQDs* boron and nitrogen co-doped single-layered graphene quantum dots, *CuNC* copper nanocluster, *CM* curcumin

proteins, and other small molecules. The ALP sensor is based on a "turn off–on" system, where the change of the LSPR band of Ag NPs causes fluorescence quenching of GQDs. Sun et al. (2018) also reported the combination between GQDs and plasmonic Au nanoflower (Au NF) for microRNA (miRNA) detection. The fluorescence of GQDs was quenched during hybridization between Au NF-ssDNA1 and GQDs-ssDNA2. The effect of distance between Au NF and GQDs provides information regarding subsequent conditions. The presence of miRNA causes the disassembly of heterodimers of Au NF@ GQDs via toehold-mediated DNA strand displacement, affording fluorescence signal recovery of the GQDs. Guerrero-Martínez et al. (2011) reported that the unique anisotropic shape of GQDs shows a strong fluorescence resonance energy transfer (FRET) behavior.

Current challenges and future perspectives

GQDs have attracted increasing attention in biosensing applications owing to their biocompatibility and excellent physical and chemical properties. The combination of GQDs with numerous nanomaterials to form nanocomposites has been proven to be a promising strategy owing to the synergistic effect in sensitivity and selectivity. This review summarizes the successful advancements of GQDs-based nanocomposites in electroanalytical and optical sensors.

Despite tremendous progress, there are still some issues that must be addressed. GQD mass production, for example, has yet to be achieved. The methods currently described allow for limited production with a wide range of sizes, shapes, and properties. GQDs prepared for one application may not be suitable for other desired applications. This is a significant disadvantage when transitioning from laboratory to real-world applications, as the manufacturing process is typically lengthy.

In addition, several challenges must be addressed to facilitate the clinical implementation of GQDs-based biosensors. To achieve high reliability and sensitivity of biosensors, the interplay between the size and shape of the recognition element and the choice of synthetic pathways of GQDs and functionalization must be understood and carefully optimized for a specific application. Even though GQD-based nanocomposites appeal to be biocompatible materials, there is no definite evidence of their safety in clinical usage. In this regard, the focus will continue on specific areas of GQDs nanocomposite applications for future in vivo biosensing research.

Furthermore, only a few studies have addressed the electron transfer process, selectivity issues, as well as the

increase in quantum yield caused by heteroatom doping and surface functionalization. Despite the fact that GQDs exhibit both excitation-dependent and excitation-independent emission spectra, another significant challenge related to the mechanism underlying their fundamental photoluminescence properties requires additional theoretical and experimental investigation.

Improvements in GQDs nanocomposite-based sensors for sensitive detection have been demonstrated in numerous recently published publications. A lot of research is being done at present to improve the analytical performance of sensors by integrating various GQDs nanocomposite combinations. The selective quantification of analytes in multiple coexisting species is necessary for the commercialization of these sensors, which remains an important challenge. Therefore, pursuant to the efforts of many researchers, the sensitivity of detection has significantly improved; nevertheless, additional study is still required to identify platforms for selective sensing.

To address these concerns, the size and surface properties of GQDs must be fine-tuned in order to fabricate highly selective and sensitive sensors. In-depth investigations into these issues will aid researchers and scientists in better understanding the electrical and optical properties of GQD-based nanocomposites, opening up new avenues for developing highly efficient biosensing platforms. Multidisciplinary collaborations could allow for the investigation of novel preparation methods and properties of GQDs and their nanocomposites for potential applications in electroanalytical and optical sensors.

Abbreviations

GQDs	Graphene quantum dots
LOD	Limit of detection
PL	Photoluminescence
SERS	Surface-enhanced Raman scattering
CV	Cyclic voltammetry
DPV	Differential pulse voltammetry
FRET	Fluorescence resonance energy transfer
GCE	Glassy carbon electrode

Acknowledgements
Not applicable.

Author contributions
MSA, DT, JL, HSJ, SCC, JHY, and DHK contributed to conceptualization; MSA and DT contributed to methodology; MSA, DT, SCC, and DHK contributed to writing—original draft preparation; and MSA, DT, JL, HSJ, SCC, JHY, and DHK contributed to writing—review, and editing. All authors have read and agreed to the published version of the manuscript.

Funding
This work was supported by the Convergence Cluster Funding (No. CCL21331-100), National Research Council of Science and Technology (NST, Korea), the Fundamental Research Program (PNK 9360) of the Korea Institute of Materials Science (KIMS), and the Basic Science Research Program through the National Research Foundation of Korea (NRF) funded by the Ministry of Education (2022R1I1A3072535).

Availability of data and materials
Not applicable.

Declarations

Competing interests
The authors declare that they have no known competing financial interests or personal relationships that could have appeared to influence the work reported in this paper.

Received: 14 April 2023 Accepted: 26 June 2023
Published online: 04 July 2023

References

Ahmadi N, Bagherzadeh M, Nemati A. Comparison between electrochemical and photoelectrochemical detection of dopamine based on titania-ceria-graphene quantum dots nanocomposite. Biosens Bioelectron. 2020;151:111977.
Anithaa VS, Shankar R, Vijayakumar S. DFT-based investigation on adsorption of methane on pristine and defected graphene. Struct Chem. 2017;28(6):1935–52.
Arumugasamy SK, Govindaraju S, Yun K. Electrochemical sensor for detecting dopamine using graphene quantum dots incorporated with multiwall carbon nanotubes. Appl Surf Sci. 2020;508:145294.
Asghari S, Mahmoudifard M. The detection of the captured circulating tumor cells on the core-shell nanofibrous membrane using hyaluronic acid-functionalized graphene quantum dots. J Biomed Mater Res B Appl Biomater. 2023;111(5):1121–32.
Bali Prasad B, Kumar A, Singh R. Synthesis of novel monomeric graphene quantum dots and corresponding nanocomposite with molecularly imprinted polymer for electrochemical detection of an anticancerous ifosfamide drug. Biosens Bioelectron. 2017;94:1–9.
Bell SEJ, Charron G, Cortes E, Kneipp J, de la Chapelle ML, Langer J, et al. Towards reliable and quantitative surface-enhanced Raman scattering (SERS): from key parameters to good analytical practice. Angew Chem Int Ed Engl. 2020;59(14):5454–62.
Biswas MC, Islam MT, Nandy PK, Hossain MM. Graphene quantum dots (GQDs) for bioimaging and drug delivery applications: a review. ACS Mater Lett. 2021;3(6):889–911.
Butler KS, Peeler DJ, Casey BJ, Dair BJ, Elespuru RK. Silver nanoparticles: correlating nanoparticle size and cellular uptake with genotoxicity. Mutagenesis. 2015;30(4):577–91.
Campuzano S, Yáñez-Sedeño P, Pingarrón JM. Carbon dots and graphene quantum dots in electrochemical biosensing. Nanomaterials. 2019;9(4):634.
Centane S, Nyokong T. Impedimetric aptasensor for HER2 biomarker using graphene quantum dots, polypyrrole and cobalt phthalocyanine modified electrodes. Sens Bio-Sens Res. 2021;34:100467.
Chakraborti H, Sinha S, Ghosh S, Pal SK. Interfacing water soluble nanomaterials with fluorescence chemosensing: graphene quantum dot to detect Hg2+ in 100% aqueous solution. Mater Lett. 2013;97:78–80.
Chandra A, Deshpande S, Shinde DB, Pillai VK, Singh N. Mitigating the cytotoxicity of graphene quantum dots and enhancing their applications in bioimaging and drug delivery. ACS Macro Lett. 2014;3(10):1064–8.
Chen C, Qiao H, Lin S, Man Luk C, Liu Y, Xu Z, et al. Highly responsive MoS2 photodetectors enhanced by graphene quantum dots. Sci Rep. 2015;5:11830.
Chen J, Wang M, Zhou X, Nie Y, Su X. Highly sensitive label-free fluorescence determination of lymphotropic virus DNA based on exonuclease assisted target recycling amplification and in-situ generation of fluorescent copper nanoclusters. Sens Actuat B Chem. 2021;326:128847.
Chen S, Hai X, Chen XW, Wang JH. In situ growth of silver nanoparticles on graphene quantum dots for ultrasensitive colorimetric detection of H(2)O(2) and glucose. Anal Chem. 2014;86(13):6689–94.
Cheng HH, Zhao Y, Fan YQ, Xie XJ, Qu LT, Shi GQ. Graphene-quantum-dot assembled nanotubes: a new platform for efficient Raman enhancement. ACS Nano. 2012;6(3):2237–44.

Choi SH. Unique properties of graphene quantum dots and their applications in photonic/electronic devices. J Phys D: Appl Phys. 2017;50(10):103002.
Chul Lim H, Jang SJ, Cho Y, Cho H, Venkataprasad G, Vinothkumar V, et al. Graphene quantum dot-doped PEDOT for simultaneous determination of ascorbic acid, dopamine, and uric acid. ChemElectroChem. 2022;9:e202200557.
Cui F, Ji J, Sun J, Wang J, Wang H, Zhang Y, et al. A novel magnetic fluorescent biosensor based on graphene quantum dots for rapid, efficient, and sensitive separation and detection of circulating tumor cells. Anal Bioanal Chem. 2019;411(5):985–95.
Dai Y, Long H, Wang X, Wang Y, Gu Q, Jiang W, et al. Versatile graphene quantum dots with tunable nitrogen doping. Part Part Syst Charact. 2014;31(5):597–604.
Das R, Parveen S, Bora A, Giri PK. Origin of high photoluminescence yield and high SERS sensitivity of nitrogen-doped graphene quantum dots. Carbon. 2020;160:273–86.
Eddin FBK, Fen YW. Recent advances in electrochemical and optical sensing of dopamine. Sensors. 2020;20:1039.
Facure MHM, Schneider R, Lima JBS, Mercante LA, Correa DS. Graphene quantum dots-based nanocomposites applied in electrochemical sensors: a recent survey. Electrochem. 2021;2(3):490–519.
Facure MHM, Schneider R, Mercante LA, Correa DS. A review on graphene quantum dots and their nanocomposites: from laboratory synthesis towards agricultural and environmental applications. Environ Sci Nano. 2020;7(12):3710–34.
Fajardo A, Tapia D, Pizarro J, Segura R, Jara P. Determination of norepinephrine using a glassy carbon electrode modified with graphene quantum dots and gold nanoparticles by square wave stripping voltammetry. J Appl Electrochem. 2019;49(4):423–32.
Fan K, Xi J, Fan L, Wang P, Zhu C, Tang Y, et al. In vivo guiding nitrogen-doped carbon nanozyme for tumor catalytic therapy. Nat Commun. 2018;9(1):1440.
Fan L, Hu Y, Wang X, Zhang L, Li F, Han D, et al. Fluorescence resonance energy transfer quenching at the surface of graphene quantum dots for ultrasensitive detection of TNT. Talanta. 2012;101:192–7.
Fan Z, Zhou S, Garcia C, Fan L, Zhou J. pH-Responsive fluorescent graphene quantum dots for fluorescence-guided cancer surgery and diagnosis. Nanoscale. 2017;9(15):4928–33.
Fei X, Liu Z, Li Y, Yang G, Su C, Zhong H, et al. One-pot green synthesis of flower-liked Au NP@GQDs nanocomposites for surface-enhanced Raman scattering. J Alloy Compd. 2017;725:1084–90.
Ganganboina AB, Dega NK, Tran HL, Darmonto W, Doong R-A. Application of sulfur-doped graphene quantum dots@ gold-carbon nanosphere for electrical pulse-induced impedimetric detection of glioma cells. Biosens Bioelectron. 2021;181:113151.
Ganganboina AB, Dutta Chowdhury A, Doong RA. N-doped graphene quantum dots-decorated V2O5 nanosheet for fluorescence turn off-on detection of cysteine. ACS Appl Mater Interfaces. 2018;10(1):614–24.
Garg M, Vishwakarma N, Sharma AL, Singh S. Amine-functionalized graphene quantum dots for fluorescence-based immunosensing of ferritin. ACS Appl Nano Mater. 2021;4(7):7416–25.
Ge J, Li Y, Wang J, Pu Y, Xue W, Liu X. Green synthesis of graphene quantum dots and silver nanoparticles compounds with excellent surface enhanced Raman scattering performance. J Alloy Compd. 2016;663:166–71.
Ghosh D, Sarkar K, Devi P, Kim K-H, Kumar P. Current and future perspectives of carbon and graphene quantum dots: from synthesis to strategy for building optoelectronic and energy devices. Renew Sustain Energy Rev. 2021;135:110391.
Gogola JL, Martins G, Gevaerd A, Blanes L, Cardoso J, Marchini FK, et al. Label-free aptasensor for p24-HIV protein detection based on graphene quantum dots as an electrochemical signal amplifier. Anal Chim Acta. 2021;1166:338548.
Goode JA, Rushworth JV, Millner PA. Biosensor regeneration: a review of common techniques and outcomes. Langmuir. 2015;31(23):6267–76.
Guerrero-Martínez A, Barbosa S, Pastoriza-Santos I, Liz-Marzán LM. Nanostars shine bright for you. Curr Opin Colloid Interface Sci. 2011;16(2):118–27.
Guo X. Surface plasmon resonance based biosensor technique: a review. J Biophotonics. 2012;5(7):483–501.
Gupta A, Kumar N. A review of mechanisms for fluorescent "'turn-on"' probes to detect Al3+ ions. RSC Adv. 2016;6(108):106413–34.
Hai X, Feng J, Chen X, Wang J. Tuning the optical properties of graphene quantum dots for biosensing and bioimaging. J Mater Chem B. 2018;6(20):3219–34.
Haque E, Kim J, Malgras V, Reddy KR, Ward AC, You J, et al. Recent advances in graphene quantum dots: synthesis, properties, and applications. Small Methods. 2018;2(10):1800050.
Hong GL, Deng HH, Zhao HL, Zou ZY, Huang KY, Peng HP, et al. Gold nanoclusters/graphene quantum dots complex-based dual-emitting ratiometric fluorescence probe for the determination of glucose. J Pharm Biomed Anal. 2020;189:113480.
Hong GL, Zhao HL, Deng HH, Yang HJ, Peng HP, Liu YH, et al. Fabrication of ultra-small monolayer graphene quantum dots by pyrolysis of trisodium citrate for fluorescent cell imaging. Int J Nanomedicine. 2018;13:4807–15.
Huang S, Qiu H, Zhu F, Lu S, Xiao Q. Graphene quantum dots as on-off-on fluorescent probes for chromium(VI) and ascorbic acid. Microchim Acta. 2015;182(9–10):1723–31.
Huang S, Wang L, Huang C, Su W, Xiao Q. Amino-functionalized graphene quantum dots based ratiometric fluorescent nanosensor for ultrasensitive and highly selective recognition of horseradish peroxidase. Sens Actuat B Chem. 2016;234:255–63.
Iannazzo D, Espro C, Celesti C, Ferlazzo A, Neri G. Smart biosensors for cancer diagnosis based on graphene quantum dots. Cancers (basel). 2021;13(13):3194.
Ji C, Zhou Y, Leblanc RM, Peng Z. Recent developments of carbon dots in biosensing: a review. ACS Sens. 2020;5(9):2724–41.
Jin J, Song W, Wang J, Li L, Tian Y, Zhu S, et al. A highly sensitive SERS platform based on small-sized Ag/GQDs nanozyme for intracellular analysis. Chem Eng J. 2022;430:132687.
Jin SH, Kim DH, Jun GH, Hong SH, Jeon S. Tuning the photoluminescence of graphene quantum dots through the charge transfer effect of functional groups. ACS Nano. 2013;7(2):1239–45.
Ju J, Chen W. Synthesis of highly fluorescent nitrogen-doped graphene quantum dots for sensitive, label-free detection of Fe (III) in aqueous media. Biosens Bioelectron. 2014;58:219–25.
Jung HS, Koh EH, Mun C, Min J, Sohng W, Chung H, et al. Hydrophobic hBN-coated surface-enhanced Raman scattering sponge sensor for simultaneous separation and detection of organic pollutants. J Mater Chem C. 2019;7(42):13059–69.
Kappen J, Bharathi S, John SA. Unusual reactivity of graphene quantum dot-wrapped silver nanoparticles with Hg(II): spontaneous growth of Hg flowers and their electrocatalytic activity. Inorg Chem. 2021;60(11):8200–10.
Kaur H, Kumar R, Babu JN, Mittal S. Advances in arsenic biosensor development—a comprehensive review. Biosens Bioelectron. 2015;63:533–45.
Kim S, Hwang SW, Kim MK, Shin DY, Shin DH, Kim CO, et al. Anomalous behaviors of visible luminescence from graphene quantum dots: interplay between size and shape. ACS Nano. 2012;6(9):8203–8.
Koh EH, Moon JY, Kim SY, Lee WC, Park SG, Kim DH, et al. A cyclodextrin-decorated plasmonic gold nanosatellite substrate for selective detection of bipyridylium pesticides. Analyst. 2021;146(1):305–14.
Lan C, Zhao J, Zhang L, Wen C, Huang Y, Zhao S. Self-assembled nanoporous graphene quantum dot-Mn3O4 nanocomposites for surface-enhanced Raman scattering based identification of cancer cells. RSC Adv. 2017;7(30):18658–67.
Langer J, Jimenez de Aberasturi D, Aizpurua J, Alvarez-Puebla RA, Auguie B, Baumberg JJ, et al. Present and Future of surface-enhanced Raman scattering. ACS Nano. 2020;14(1):28–117.
Lee NE, Jeong J-M, Lim HS, Lee SY, Cho SO. Ultraviolet/blue light emitting high-quality graphene quantum dots and their biocompatibility. Carbon. 2020;170:213–9.
Li L, Wu G, Yang G, Peng J, Zhao J, Zhu JJ. Focusing on luminescent graphene quantum dots: current status and future perspectives. Nanoscale. 2013a;5(10):4015–39.
Li M, Chen T, Gooding JJ, Liu J. Review of carbon and graphene quantum dots for sensing. ACS Sens. 2019a;4(7):1732–48.
Li M, Chen T, Gooding JJ, Liu J. Review of carbon and graphene quantum dots for sensing. ACS Sens. 2019b;4(7):1732–48.
Li RS, Yuan B, Liu JH, Liu ML, Gao PF, Li YF, et al. Boron and nitrogen co-doped single-layered graphene quantum dots: a high-affinity platform for visualizing the dynamic invasion of HIV DNA into living cells

through fluorescence resonance energy transfer. J Mater Chem B. 2017;5(44):8719–24.
Li X, Zhu S, Xu B, Ma K, Zhang J, Yang B, et al. Self-assembled graphene quantum dots induced by cytochrome c: a novel biosensor for trypsin with remarkable fluorescence enhancement. Nanoscale. 2013b;5(17):7776–9.
Li Z, Wang Y, Ni Y, Kokot S. A rapid and label-free dual detection of Hg (II) and cysteine with the use of fluorescence switching of graphene quantum dots. Sens Actuat B Chem. 2015;207:490–7.
Liang X, Li N, Zhang R, Yin P, Zhang C, Yang N, et al. Carbon-based SERS biosensor: from substrate design to sensing and bioapplication. NPG Asia Mater. 2021;13(1):8.
Liaquat H, Imran M, Latif S, Hussain N, Bilal M. Multifunctional nanomaterials and nanocomposites for sensing and monitoring of environmentally hazardous heavy metal contaminants. Environ Res. 2022;214(Pt 1):113795.
Linh VTN, Moon J, Mun C, Devaraj V, Oh J-W, Park S-G, et al. A facile low-cost paper-based SERS substrate for label-free molecular detection. Sens Actuat B Chem. 2019a;291:369–77.
Linh VTN, Xiao X, Jung HS, Giannini V, Maier SA, Kim DH, et al. Compact integration of TiO(2) nanoparticles into the cross-points of 3D vertically stacked Ag nanowires for plasmon-enhanced photocatalysis. Nanomaterials (Basel). 2019b;9(3):468.
Linh VTN, Yim S-G, Mun C, Yang J-Y, Lee S, Yoo YW, et al. Bioinspired plasmonic nanoflower-decorated microneedle for label-free intradermal sensing. Appl Surf Sci. 2021;551:149411.
Liu D, Chen X, Hu Y, Sun T, Song Z, Zheng Y, et al. Raman enhancement on ultra-clean graphene quantum dots produced by quasi-equilibrium plasma-enhanced chemical vapor deposition. Nat Commun. 2018a;9(1):193.
Liu JH, Li RS, Yuan B, Wang J, Li YF, Huang CZ. Mitochondria-targeting single-layered graphene quantum dots with dual recognition sites for ATP imaging in living cells. Nanoscale. 2018b;10(36):17402–8.
Liu JJ, Zhang XL, Cong ZX, Chen ZT, Yang HH, Chen GN. Glutathione-functionalized graphene quantum dots as selective fluorescent probes for phosphate-containing metabolites. Nanoscale. 2013;5(5):1810–5.
Liu R, Yang R, Qu C, Mao H, Hu Y, Li J, et al. Synthesis of glycine-functionalized graphene quantum dots as highly sensitive and selective fluorescent sensor of ascorbic acid in human serum. Sens Actuat B Chem. 2017a;241:644–51.
Liu W-T, Wu SW, Schuck PJ, Salmeron M, Shen YR, Wang F. Nonlinear broadband photoluminescence of graphene induced by femtosecond laser irradiation. Phys Rev B. 2010;82(8):081408(R).
Liu X, Li Y, Xue W, Ge J, Wang J, Sun J. 3D nano-arrays of silver nanoparticles and graphene quantum dots with excellent surface-enhanced Raman scattering. Mater Sci Technol. 2017b;34(6):679–87.
Lu H-F, Zhang M-M, Wu D, Huang J-L, Zhu L-L, Wang C-M, et al. Colorimetric and fluorescent dual-mode sensing of alkaline phosphatase activity in L-02 cells and its application in living cell imaging based on in-situ growth of silver nanoparticles on graphene quantum dots. Sens Actuat B Chem. 2018;258:461–9.
Magar HS, Hassan RY, Mulchandani A. Electrochemical impedance spectroscopy (EIS): principles, construction, and biosensing applications. Sensors. 2021;21(19):6578.
Mansuriya BD, Altintas Z. Graphene quantum dot-based electrochemical immunosensors for biomedical applications. Materials. 2019;13(1):96.
Mansuriya BD, Altintas Z. Applications of graphene quantum dots in biomedical sensors. Sensors. 2020;20(4):1072.
Mansuriya BD, Altintas Z. Enzyme-free electrochemical nano-immunosensor based on graphene quantum dots and gold nanoparticles for cardiac biomarker determination. Nanomaterials. 2021;11(3):578.
Mars A, Hamami M, Bechnak L, Patra D, Raouafi N. Curcumin-graphene quantum dots for dual mode sensing platform: electrochemical and fluorescence detection of APOe4, responsible of Alzheimer's disease. Anal Chim Acta. 2018;1036:141–6.
Mary YS, Mary YS. Utilization of doped/undoped graphene quantum dots for ultrasensitive detection of duphaston, a SERS platform. Spectrochim Acta A Mol Biomol Spectrosc. 2021;244:118865.
Mehata MS, Biswas S. Synthesis of fluorescent graphene quantum dots from graphene oxide and their application in fabrication of GQDs@AgNPs nanohybrids and sensing of H2O2. Ceram Int. 2021;47(13):19063–72.
Miao X, Wen S, Su Y, Fu J, Luo X, Wu P, et al. Graphene quantum dots wrapped gold nanoparticles with integrated enhancement mechanisms as sensitive and homogeneous substrates for surface-enhanced Raman spectroscopy. Anal Chem. 2019;91(11):7295–303.
Minteer SD. Advances in electroanalytical chemistry. J Am Chem Soc. 2018;140:2701–3.
Mollarasouli F, Serafín V, Campuzano S, Yáñez-Sedeño P, Pingarrón JM, Asadpour-Zeynali K. Ultrasensitive determination of receptor tyrosine kinase with a label-free electrochemical immunosensor using graphene quantum dots-modified screen-printed electrodes. Anal Chim Acta. 2018;1011:28–34.
Motahari S, Shayeganfar F, Neek-Amal M. Van der Waals energy surface of a carbon nanotube sheet. Solid State Commun. 2012;152(3):225–30.
Mueller ML, Yan X, McGuire JA, Li LS. Triplet States and electronic relaxation in photoexcited graphene quantum dots. Nano Lett. 2010;10(7):2679–82.
Nemati F, Zare-Dorabei R, Hosseini M, Ganjali MR. Fluorescence turn-on sensing of thiamine based on Arginine–functionalized graphene quantum dots (Arg-GQDs): central composite design for process optimization. Sens Actuat B Chem. 2018;255:2078–85.
Nguyen HH, Lee SH, Lee UJ, Fermin CD, Kim M. Immobilized enzymes in biosensor applications. Materials (basel). 2019;12(1):121.
Nxele SR, Nyokong T. The effects of the composition and structure of quantum dots combined with cobalt phthalocyanine and an aptamer on the electrochemical detection of prostate specific antigen. Dyes Pigm. 2021;192:109407.
Ozhukil Valappil M, Pillai VK, Alwarappan S. Spotlighting graphene quantum dots and beyond: synthesis, properties and sensing applications. Appl Mater Today. 2017;9:350–71.
Pandit S, Kunwar S, Kulkarni R, Mandavka R, Lin S, Lee J. Fabrication of hybrid Pd@Ag core-shell and fully alloyed bi-metallic AgPd NPs and SERS enhancement of Rhodamine 6G by a unique mixture approach with graphene quantum dots. Appl Surf Sci. 2021;548:149252.
Pei H, Zhu S, Yang M, Kong R, Zheng Y, Qu F. Graphene oxide quantum dots@ silver core-shell nanocrystals as turn-on fluorescent nanoprobe for ultrasensitive detection of prostate specific antigen. Biosens Bioelectron. 2015;74:909–14.
Perez-Jimenez AI, Lyu D, Lu Z, Liu G, Ren B. Surface-enhanced Raman spectroscopy: benefits, trade-offs and future developments. Chem Sci. 2020;11(18):4563–77.
Perini G, Palmieri V, Ciasca G, De Spirito M, Papi M. Unravelling the potential of graphene quantum dots in biomedicine and neuroscience. Int J Mol Sci. 2020;21(10):3712.
Pinilla-Penalver E, Garcia-Bejar B, Contento AM, Rios A. Graphene quantum dots an efficient nanomaterial for enhancing the photostability of trans-resveratrol in food samples. Food Chem. 2022;386:132766.
Pirzada M, Altintas Z. Nanomaterials for healthcare biosensing applications. Sensors (basel). 2019;19(23):5311.
Plou J, Charconnet M, Garcia I, Calvo J, Liz-Marzan LM. Preventing memory effects in surface-enhanced Raman scattering substrates by polymer coating and laser-activated deprotection. ACS Nano. 2021;15(5):8984–95.
Pustovit VN, Shahbazyan TV. SERS from molecules adsorbed on small Ag nanoparticles: a microscopic model. Chem Phys Lett. 2006;420:469–73.
Qu Z, Li N, Na W, Su X. A novel fluorescence "turn off–on" nanosensor for sensitivity detection acid phosphatase and inhibitor based on glutathione-functionalized graphene quantum dots. Talanta. 2019;192:61–8.
Reshma VG, Mohanan PV. Quantum dots: applications and safety consequences. J Lumin. 2019;205:287–98.
Ryu J, Lee E, Lee K, Jang J. A graphene quantum dots based fluorescent sensor for anthrax biomarker detection and its size dependence. J Mater Chem B. 2015;3(24):4865–70.
Saisree S, JS AN, Sandhya K. A highly stable copper nano cluster on nitrogen-doped graphene quantum dots for the simultaneous electrochemical sensing of dopamine, serotonin, and nicotine: a possible addiction scrutinizing strategy. J Mater Chem B. 2022;10(21):3974–88.
Salehnia F, Faridbod F, Dezfuli AS, Ganjali MR, Norouzi P. Cerium(III) ion sensing based on graphene quantum dots fluorescent turn-off. J Fluoresc. 2017;27(1):331–8.
Sapkota B, Benabbas A, Lin HG, Liang W, Champion P, Wanunu M. Peptide-decorated tunable-fluorescence graphene quantum dots. ACS Appl Mater Interfaces. 2017;9(11):9378–87.

Savas S, Altintas Z. Graphene quantum dots as nanozymes for electrochemical sensing of Yersinia enterocolitica in milk and human serum. Materials. 2019;12(13):2189.
Serebrennikova KV, Berlina AN, Sotnikov DV, Zherdev AV, Dzantiev BB. Raman scattering-based biosensing: new prospects and opportunities. Biosensors (basel). 2021;11(12):512.
Shang L, Nienhaus K, Nienhaus GU. Engineered nanoparticles interacting with cells: size matters. J Nanobiotechnol. 2014;12:5.
Sharifi M, Avadi MR, Attar F, Dashtestani F, Ghorchian H, Rezayat SM, et al. Cancer diagnosis using nanomaterials based electrochemical nanobiosensors. Biosens Bioelectron. 2019;126:773–84.
Shen J, Zhu Y, Chen C, Yang X, Li C. Facile preparation and upconversion luminescence of graphene quantum dots. Chem Commun (camb). 2011;47(9):2580–2.
Shi H, Chen L, Niu N. An off-on fluorescent probe based on graphene quantum dots intercalated hydrotalcite for determination of ascorbic acid and phytase. Sens Actuat B Chem. 2021;345:130353.
Shi J, Lyu J, Tian F, Yang M. A fluorescence turn-on biosensor based on graphene quantum dots (GQDs) and molybdenum disulfide (MoS2) nanosheets for epithelial cell adhesion molecule (EpCAM) detection. Biosens Bioelectron. 2017;93:182–8.
Sinduja B, John SA. Ultrasensitive optical sensor for hydrogen peroxide using silver nanoparticles synthesized at room temperature by GQDs. Sens Actuat B Chem. 2017;247:648–54.
Sinduja B, John SA. Highly selective naked eye detection of vitamin B1 in the presence of other vitamins using graphene quantum dots capped gold nanoparticles. New J Chem. 2019;43(5):2111–7.
Sireesha M, Jagadeesh Babu V, Kranthi Kiran AS, Ramakrishna S. A review on carbon nanotubes in biosensor devices and their applications in medicine. Nanocomposites. 2018;4(2):36–57.
Sk MA, Ananthanarayanan A, Huang L, Lim KH, Chen P. Revealing the tunable photoluminescence properties of graphene quantum dots. J Mater Chem C. 2014;2(34):6954–60.
Song L, Shi J, Lu J, Lu C. Structure observation of graphene quantum dots by single-layered formation in layered confinement space. Chem Sci. 2015;6(8):4846–50.
Sun J, Cui F, Zhang R, Gao Z, Ji J, Ren Y, et al. Comet-like heterodimers "Gold Nanoflower @Graphene Quantum Dots" probe with FRET "Off" to DNA circuit signal "On" for sensing and imaging microRNA in vitro and in vivo. Anal Chem. 2018;90(19):11538–47.
Tabish TA, Hayat H, Abbas A, Narayan RJ. Graphene quantum dot–based electrochemical biosensing for early cancer detection. Curr Opin Electrochem. 2021;30:100786.
Tabish TA, Zhang S (2016) Graphene quantum dots: syntheses, properties, and biological applications. Comprehensive Nanoscience and Nanotechnology, pp 171–192
Tagit O, Hildebrandt N. Fluorescence sensing of circulating diagnostic biomarkers using molecular probes and nanoparticles. ACS Sens. 2017;2(1):31–45.
Tajik S, Dourandish Z, Zhang K, Beitollahi H, Van Le Q, Jang HW, et al. Carbon and graphene quantum dots: a review on syntheses, characterization, biological and sensing applications for neurotransmitter determination. RSC Adv. 2020;10(26):15406–29.
Tang S, Yu C, Qian L, Zhou C, Zhen Z, Liu B, et al. Nitrogen-doped graphene quantum dots-MoS2 nanoflowers as a fluorescence sensor with an off/on switch for intracellular glutathione detection and fabrication of molecular logic gates. Microchem J. 2021;171:106786.
Tang Y, Su Y, Yang N, Zhang L, Lv Y. Carbon nitride quantum dots: a novel chemiluminescence system for selective detection of free chlorine in water. Anal Chem. 2014;86(9):4528–35.
Tashkhourian J, Nami-Ana SF, Shamsipur M. Designing a modified electrode based on graphene quantum dot-chitosan application to electrochemical detection of epinephrine. J Mol Liq. 2018;266:548–56.
Thanomsak S, Insombat C, Chaiyo P, Tuntulani T, Janrungroatsakul W. Fabrication of a paper-based sensor from graphene quantum dots coated with a polymeric membrane for the determination of gold(III) ions. Anal Methods. 2021;13(40):4785–92.
Thirumalai D, Kim S, Kim S, Chang S-C. Reagentless amperometric pyruvate biosensor based on a Prussian blue-and enzyme nanoparticle-modified screen-printed carbon electrode. ACS Omega. 2020;5(46):30123–9.
Tian J, Wei W, Wang J, Ji S, Chen G, Lu J. Fluorescence resonance energy transfer aptasensor between nanoceria and graphene quantum dots for the determination of ochratoxin A. Anal Chim Acta. 2018;1000:265–72.
Tran HL, Dega NK, Lu S-M, Huang Y-F, Doong R-A. Ultrasensitive detection of breast cancer cells with a lectin-based electrochemical sensor using N-doped graphene quantum dots as the sensing probe. Sens Actuat B. 2022;368:132233.
Umrao S, Jang M-H, Oh J-H, Kim G, Sahoo S, Cho Y-H, et al. Microwave bottom-up route for size-tunable and switchable photoluminescent graphene quantum dots using acetylacetone: new platform for enzyme-free detection of hydrogen peroxide. Carbon. 2015;81:514–24.
Valley N, Greeneltch N, Van Duyne RP, Schatz GC. A look at the origin and magnitude of the chemical contribution to the enhancement mechanism of surface-enhanced Raman spectroscopy (SERS): theory and experiment. J Phys Chem Lett. 2013;4(16):2599–604.
Wadhera T, Kakkar D, Wadhwa G, Raj B. Recent advances and progress in development of the field effect transistor biosensor: a review. J Electron Mater. 2019;48(12):7635–46.
Wang F, Gu Z, Lei W, Wang W, Xia X, Hao Q. Graphene quantum dots as a fluorescent sensing platform for highly efficient detection of copper(II) ions. Sens Actuat B Chem. 2014;190:516–22.
Wang L, Zhu S-J, Wang H-Y, Wang Y-F, Hao Y-W, Zhang J-H, et al. Unraveling bright molecule-like state and dark intrinsic state in green-fluorescence graphene quantum dots via ultrafast spectroscopy. Adv Opt Mater. 2013;1(3):264–71.
Wang S, Cole IS, Zhao D, Li Q. The dual roles of functional groups in the photoluminescence of graphene quantum dots. Nanoscale. 2016;8(14):7449–58.
Wang Y-X, Rinawati M, Zhan J-D, Lin K-Y, Huang C-J, Chen K-J, et al. Boron-doped graphene quantum dots anchored to carbon nanotubes as noble metal-free electrocatalysts of uric acid for a wearable sweat sensor. ACS Appl Nano Mater. 2022;5(8):11100–10.
Wei M, Tian D, Liu S, Zheng X, Duan S, Zhou C. β-Cyclodextrin functionalized graphene material: a novel electrochemical sensor for simultaneous determination of 2-chlorophenol and 3-chlorophenol. Sens Actuat B Chem. 2014;195:452–8.
Wolfbeis OS. An overview of nanoparticles commonly used in fluorescent bioimaging. Chem Soc Rev. 2015;44(14):4743–68.
Wu C, Wang C, Han T, Zhou X, Guo S, Zhang J. Insight into the cellular internalization and cytotoxicity of graphene quantum dots. Adv Healthc Mater. 2013;2(12):1613–9.
Wu C, Yuan Y, He Q, Song R. Two-step synthesis of Ag@GQD hybrid with enhanced photothermal effect and catalytic performance. Nanotechnology. 2016;27(48):48LT02.
Wu M, Guo H, Liu L, Liu Y, Xie L. Size-dependent cellular uptake and localization profiles of silver nanoparticles. Int J Nanomed. 2019;14:4247–59.
Xiaoyan Z, Ruiyi L, Zaijun L, Zhiguo G, Guangli W. Ultrafast synthesis of gold/proline-functionalized graphene quantum dots and its use for ultrasensitive electrochemical detection of p-acetamidophenol. RSC Adv. 2016;6(48):42751–5.
Xie R, Wang Z, Zhou W, Liu Y, Fan L, Li Y, et al. Graphene quantum dots as smart probes for biosensing. Anal Methods. 2016;8(20):4001–16.
Xu J, Wang Y, Hu S. Nanocomposites of graphene and graphene oxides: synthesis, molecular functionalization and application in electrochemical sensors and biosensors. A review. Microchim Acta. 2017;184(1):1–44.
Xu Q, Yuan H, Dong X, Zhang Y, Asif M, Dong Z, et al. Dual nanoenzyme modified microelectrode based on carbon fiber coated with AuPd alloy nanoparticles decorated graphene quantum dots assembly for electrochemical detection in clinic cancer samples. Biosens Bioelectron. 2018;107:153–62.
Yan C, Hu X, Guan P, Hou T, Chen P, Wan D, et al. Highly biocompatible graphene quantum dots: green synthesis, toxicity comparison and fluorescence imaging. J Mater Sci. 2019;55(3):1198–215.
Yan Y, Chen J, Li N, Tian J, Li K, Jiang J, et al. Systematic bandgap engineering of graphene quantum dots and applications for photocatalytic water splitting and CO2 reduction. ACS Nano. 2018;12(4):3523–32.
Yola ML, Atar N. A novel detection approach for serotonin by graphene quantum dots/two-dimensional (2D) hexagonal boron nitride nanosheets with molecularly imprinted polymer. Appl Surf Sci. 2018;458:648–55.

Zhang H, Wang Y, Zhao D, Zeng D, Xia J, Aldalbahi A, et al. Universal fluorescence biosensor platform based on graphene quantum dots and pyrene-functionalized molecular beacons for detection of microRNAs. ACS Appl Mater Interfaces. 2015a;7(30):16152–6.
Zhang N, Ma W, Han D, Wang L, Wu T, Niu L. The fluorescence detection of glutathione by OH radicals' elimination with catalyst of MoS2/rGO under full spectrum visible light irradiation. Talanta. 2015b;144:551–8.
Zhang X, Wang H, Wang H, Zhang Q, Xie J, Tian Y, et al. Single-layered graphitic-C(3)N(4) quantum dots for two-photon fluorescence imaging of cellular nucleus. Adv Mater. 2014;26(26):4438–43.
Zhang X, Wei C, Li Y, Yu D. Shining luminescent graphene quantum dots: synthesis, physicochemical properties, and biomedical applications. TrAC, Trends Anal Chem. 2019;116:109–21.
Zhao H, Guo Y, Zhu S, Song Y, Jin J, Ji W, et al. Facile synthesis of silver nanoparticles/carbon dots for a charge transfer study and peroxidase-like catalytic monitoring by surface-enhanced Raman scattering. Appl Surf Sci. 2017;410:42–50.
Zheng XT, Ananthanarayanan A, Luo KQ, Chen P. Glowing graphene quantum dots and carbon dots: properties, syntheses, and biological applications. Small. 2015;11(14):1620–36.
Zhou X, Gao X, Song F, Wang C, Chu F, Wu S. A sensing approach for dopamine determination by boronic acid-functionalized molecularly imprinted graphene quantum dots composite. Appl Surf Sci. 2017;423:810–6.
Zhu S, Zhang J, Qiao C, Tang S, Li Y, Yuan W, et al. Strongly green-photoluminescent graphene quantum dots for bioimaging applications. Chem Commun (camb). 2011;47(24):6858–60.
Zhu SJ, Song YB, Zhao XH, Shao JR, Zhang JH, Yang B. The photoluminescence mechanism in carbon dots (graphene quantum dots, carbon nanodots, and polymer dots): current state and future perspective. Nano Res. 2015;8(2):355–81.
Zhuo SJ, Shao MW, Lee ST. Upconversion and downconversion fluorescent graphene quantum dots: ultrasonic preparation and photocatalysis. ACS Nano. 2012;6(2):1059–64.
Zou F, Zhou H, Tan TV, Kim J, Koh K, Lee J. Dual-mode SERS-fluorescence immunoassay using graphene quantum dot labeling on one-dimensional aligned magnetoplasmonic nanoparticles. ACS Appl Mater Interfaces. 2015;7(22):12168–75.

Publisher's Note